

STUDY OF EFFECT OF PLACEMENT OF GROUYNE ON SHARP BEND IN RIVER USING CFD ANALYSIS

A Dissertation submitted in partial fulfillment of the requirement for the
Award of degree of

MASTER OF TECHNOLOGY IN HYDRAULICS & WATER RESOURCES ENGINEERING BY

KIRTI SINGH
(2K15/HFE/10)

Under the Guidance of

Mr. Bharat Jhamnani
Assistant Professor
Department of Civil Engineering
Delhi Technological University
Delhi



**DELHI TECHNOLOGICAL UNIVERSITY
(FORMERLY DELHI COLLEGE OF ENGINEERING)**

DELHI – 110042

July-2017



CANDIDATE'S DECLARATION

I do hereby certify that the work presented is the report entitled “**STUDY OF EFFECT OF PLACEMENT OF GROUYNE ON SHARP BEND IN RIVER USING CFD ANALYSIS**” in the partial fulfillment of the requirements for the award of the degree of “Master of Technology” in Hydraulics & Water Resources Engineering submitted in the Department of Civil Engineering, Delhi Technological University, is an authentic record of our own work carried out under the supervision of Mr. Bharat Jhamnani (Assistant Professor), Department of Civil Engineering.

I have not submitted the matter embodied in the report for the award of any other degree or diploma.

Kirti Singh

Date:

(2K15/HFE/10)

CERTIFICATE

This is to certify that above statement made by the candidate is correct to best of my knowledge.

Mr. Bharat Jhamnani
(Assistant Professor)
Department of Civil Engineering
Delhi Technological University
Delhi

ACKNOWLEDGEMENT

I take this opportunity to express my profound gratitude and deep regards to Mr. Bharat Jhamnani (Assistant Professor, Civil Engineering Department, DTU) for his exemplary guidance, monitoring and constant encouragement throughout the course of this project work. The blessing, help and guidance given by him from time to time shall carry me a long way in life on which I am going to embark.

I would also like to thank Dr. Nirender Dev (Head of Department, Civil Engineering, DTU) for extending his support and guidance.

Professors and faculties of the Department of Civil Engineering, DTU, have always extended their full co-operation and help. They have been kind enough to give their opinions on the project matter; I am deeply obliged to them. They have been a source of encouragement and have continuously been supporting me with their knowledge base, during the study. Several of well-wishers extended their help to me directly or indirectly and we are grateful to all of them without whom it would have been impossible for me to carry on my work.

ABSTRACT

In a meandering river the most basic segment of the river is the point at which it changes its curvature, at this segment complex flow happens, also the additional forces like centrifugal force that become possibly the most important factor because of the curvature make the bank protection against scouring essential. As there are not much examination that focus on the investigation of flow in a channel bend, inferable from the complexities. Reenacting the shape and waterway conditions in a flume is likewise intense, fortunately making utilization of computational dynamic programming help in simulation studies. Groynes are usually installed along the river side and those are used for a lot of application such as bank protection. These structures would change the flow pattern and prevent bank erosion. So understanding turbulent flow pattern around groynes for designing groyne installation criteria is very important. In this subcritical flow pattern around an indirect groyne in different angle of installation was established and 3D simulations in Fluent software have been applied to investigate the effect of angle of groyne installation on separation zone length behind it. In this examination groyne at various positions on the channel bend are investigated utilizing ANSYS Fluent software. The turbulence model used was standard k-epsilon model for the flow. In all cases the channel width and inlet flow depth were constant and the bed slope of the channel was zero. The tip velocities, protected length and bed shear stress were compared for different positions of groyne. The most effective position of the groyne among the different cases was suggested in this study, also suggestions were made for the appropriate length of groyne.

CONTENTS

Title	Page No.
CANDIDATE'S DECLARATION	ii
ACKNOWLEDGEMENT	iii
ABSTRACT	iv
LIST OF FIGURES	vii
LIST OF TABLES	x
LIST OF SYMBOLS	xi
1. INTRODUCTION	1
1.1. INTRODUCTION	1
1.2. MEANDERING OF RIVER	1
1.3. BACKGROUND	2
1.4. OBJECTIVES OF STUDY	3
1.5. COMPUTATIONAL FLUID DYNAMICS	4
1.6. RESEARCH STRATEGY	4
1.7. RESEARCH CONSTRAINT	5
1.8. ORGANIZATION OF DISSERTATION	5
2. LITERATURE REVIEW	6
2.1. GROYNES	6
2.2. SIGNIFICANCE AND WORKING OF GROYNES	6
2.3. SIGNIFICANCE OF POSITION OF GROYNES	6
2.4. OBJECTIVES OF GROYNES	7
2.5. TYPES OF GROYNE	7
2.6. SEDIMENT TRANSPORT	8
2.7. STATUS OF RESEARCH WORK	10
3. METHODOLOGY	17
3.1. INTRODUCTION	17
3.2. DESCRIPTION OF HYPOTHETICAL CHANNEL MODEL	17
3.2.1. CHANNEL CHARACTERISRICS	17
3.2.2. GROYNE CHARACTERISTICS	18
3.3. POSITION OF GROYNE FOR STUDY	18
3.4. INPUT VARIABLES	19
3.5. MEASUREMENTS	19
3.5.1. PROTECTED LENGTH	19
3.5.2. VELOCITY	19
3.5.3. SHEAR STRESS	20
3.6. COMPUTATIONAL FLUID DYNAMICS AND GOVERNING EQUATIONS	20

3.7. SOFTWARE INPUT	21
3.7.1. GEOMETRY	21
3.7.2. MESHING	22
3.7.3. SETUP	23
3.7.4. SOLUTION	24
4. RESULTS AND ANALYSIS	
4.1. INTRODUCTION	26
4.2. SOFTWARE OUTPUT	26
4.3. PLOTS OBTAINED FROM ANSYS FLUENT (CFD –POST)	39
4.3.1. STREAMLINES	40
4.3.2. VELOCITY VECTORS	42
4.3.3. CONTOURS OF VELOCITY	44
4.3.4. CONTOURS OF BED SHEAR STRESS	46
4.4. VARIATION OF FACTOR D/L WITH FACTOR L/B FOR DIFFERENT POSITION OF GROUYNE	49
4.5. VARIATION OF FACTOR L/B WITH FACTOR V_{tip}/V_{app} FOR DIFFERENT POSITION OF GROUYNE	51
4.6. VARIATION OF FACTOR τ_{max} FOR DIFFERENT GROUYNE POSITIONS	52
4.7. SUMMARY	57
5. CONCLUSIONS	59
5.1. INTRODUCTION	59
5.2. SUGGESTION FOR THE BEST PLACEMENT OF GROUYNE	60
5.3. FURTHER IMPROVEMENTS	60
6. REFERENCES	61

LIST OF FIGURES

Figure No.	Title	Page No.
Fig. No. 1	Helical flow in bend	3
Fig. No. 2	Classification of groynes by action on stream flow	8
Fig. No. 3	Classification of groynes by appearance in plan view	8
Fig. No. 4	Orientation of groyne placement	18
Fig. No. 5	Dialog box showing basic components of Ansys Fluent.	21
Fig. No. 6	Channel Geometry as it looks in Design Modular of Ansys Fluent	22
Fig. No. 7	Meshing by Cut Cell Assembly method with relevance to proximity and curvature.	22
Fig. No. 8	Definition of mathematical model used, k-epsilon	23
Fig. No. 9	One of the case of this study where the solution converged at 213th iteration	25
Fig. No. 10	Streamlines for groyne position “A” having groyne at 15°, with respect to decided meridian “OA”.	40
Fig. No. 11	Streamlines for groyne position “A” having groyne at 30°, with respect to decided meridian “OA”.	40
Fig. No. 12	Streamlines for groyne position “A” having groyne at 45°, with respect to decided meridian “OA”.	41
Fig. No. 13	Streamlines for groyne position “A” having groyne at 60°, with respect to decided meridian “OA”.	41
Fig. No. 14	Velocity Vectors for groyne position “A” having groyne at 15°, with respect to decided meridian “OA”.	42
Fig. No. 15	Velocity Vectors for groyne position “A” having groyne at 30°, with respect to decided meridian “OA”.	42
Fig. No. 16	Velocity Vectors for groyne position “A” having groyne at 45°, with respect to decided meridian “OA”.	43

Fig. No. 17	Velocity Vectors for groyne position “A” having groyne at 60°, with respect to decided meridian “OA”.	43
Fig. No. 18	Velocity Contours for groyne position “A” having groyne at 15°, with respect to decided meridian “OA”.	44
Fig. No. 19	Velocity Contours for groyne position “A” having groyne at 30°, with respect to decided meridian “OA”.	44
Fig. No. 20	Velocity Contours for groyne position “A” having groyne at 45°, with respect to decided meridian “OA”.	45
Fig. No. 21	Velocity Contours for groyne position “A” having groyne at 60°, with respect to decided meridian “OA”.	45
Fig. No. 22	Bed Shear Stress Contours for groyne position “A” having groyne at 15°, with respect to decided meridian “OA”.	46
Fig. No. 23	Bed Shear Stress Contours for groyne position “A” having groyne at 30°, with respect to decided meridian “OA”.	46
Fig. No. 24	Bed Shear Stress Contours for groyne position “A” having groyne at 45°, with respect to decided meridian “OA”.	47
Fig. No. 25	Bed Shear Stress Contours for groyne position “A” having groyne at 60°, with respect to decided meridian “OA”.	47
Fig. No. 26	Variation of D/L with L/B for Velocity 1m/s	49
Fig. No. 27	Variation of D/L with L/B for Velocity 1.5m/s	49
Fig. No. 28	Variation of D/L with L/B for Velocity 2m/s	50
Fig. No. 29	Variation of V_{tip}/V_{app} with L/B for velocity 1 m/s.	51
Fig. No. 30	Variation of V_{tip}/V_{app} with L/B for velocity 1.5 m/s.	51
Fig. No. 31	Variation of V_{tip}/V_{app} with L/B for velocity 2 m/s.	52
Fig. No. 32	For position 1, τ_{max} for groyne size L=3m, B=0.5 for velocity 1m/s	53
Fig. No. 33	For position 1, τ_{max} for groyne size L=3m, B=0.5 for velocity 1.5m/s	53
Fig. No. 34	For position 1, τ_{max} for groyne size L=3m, B=0.5 for velocity 2m/s	54
Fig. No. 35	For position 2, τ_{max} for groyne size L=3m, B=0.5 for velocity 1m/s	54
Fig. No. 36	For position 2, τ_{max} for groyne size L=3m, B=0.5 for	55

	velocity 1.5m/s	
Fig. No. 37	For position 2 , τ_{\max} for groyne size L=3m, B=0.5 for velocity 2m/s	55
Fig. No. 38	For position 3 , τ_{\max} for groyne size L=3m, B=0.5 for velocity 1m/s	56
Fig. No. 39	For position 3 , τ_{\max} for groyne size L=3m, B=0.5 for velocity 1.5m/s	56
Fig. No. 40	For position 3 , τ_{\max} for groyne size L=3m, B=0.5 for velocity 2m/s	57

LIST OF TABLE

Table No.	Title	Page No.
Table 1	CHANNEL AND GROUYNE DESCRIPTION	3
Table 2	Position of different groyne at concave face	19
Table 3	Meshing Components and the assigned values/method for study.	23
Table 4	Boundary Conditions for each case of observation	24
Table 5	Solution Methods used in this study	25
Table 6	For position A (<u>UPSTREAM ARC</u>)	28
Table 7	For position B (<u>1/4th UPSTREAM ARC</u>)	29
Table 8	For position C (<u>1/2 UPSTREAM ARC</u>)	30
Table 9	For position A (<u>UPSTREAM ARC</u>)	31
Table 10	For position B (<u>1/4th UPSTREAM ARC</u>)	32
Table 11	For position C (<u>1/2 UPSTREAM ARC</u>)	33
Table12	For position A (<u>UPSTREAM ARC</u>)	34
Table 13	For position B (<u>1/4th UPSTREAM ARC</u>)	35
Table 14	For position C (<u>1/2 UPSTREAM ARC</u>)	36
Table 15	For position A (upstream arc) GROUYNE L=3, B=0.5, approach velocity=1m/s.	37
Table 16	For position A (upstream arc) GROUYNE L=4, B=0.2, approach velocity=1.5m/s.	37
Table 17	For position A (upstream arc) GROUYNE L=3, B=0.5, approach velocity=2m/s.	38
Table 18	For position B (1/4 th upstream arc) GROUYNE L=3, B=0.5, approach velocity=1m/s.	38
Table 19	For position B (1/4 th upstream arc) GROUYNE L=3.5, B=0.5, approach velocity=1.5m/s.	38
Table 20	For position B (1/4 th upstream arc) GROUYNE L=3, B=0.5, approach velocity=2m/s.	39
Table 21	For position C (1/2 upstream arc) GROUYNE L=3, B=0.5, approach velocity=1m/s.	39
Table 22	For position C (1/2 upstream arc) GROUYNE L=3, B=0.5, approach velocity=1.5m/s.	39
Table 23	For position C (1/2 upstream arc) GROUYNE L=3, B=0.5, approach velocity=2m/s.	40

LIST OF SYMBOLS

Symbol	Title
S_r	Surface Slope
g	Gravitational acceleration
V_{app}	Velocity of approach
V_{tip}	Tip velocity
τ_{max}	Maximum bed shear stress
τ_o	Initial (undisturbed) bed shear stress
D	Protected length
L	Length of groyne
V_{max}	Absolute maximum velocity
R	Mean radius of curvature

CHAPTER 1

INTRODUCTION

1.1. INTRODUCTION

In natural channels and bodies of water the bed is not fixed but is composed of mobile particles; e.g. gravel, sand or silt. These may be dislodged and moved by the flow – the process of *sediment transport*. These sediments travel from the river to various reservoirs which reduce the storage capacity of the reservoir, reduces the navigation depth, and changes the path of river. This makes the river to meander.

1.2. MEANDERING OF RIVER

When there is heavy sediment load in the river water, which is more than that required for stability, river tends to build up a steeper slope by depositing the sediment load on the bed. If the banks are not resistant to erosion, increased velocity may erode the banks. Consequently the river flow may be deviated from its axis and meanders are formed.

If the equilibrium condition (stable condition) of the river is somehow disturbed and if the bed is not degradable, the banks get eroded. Unequal erosion of the banks may deviate the flow from its axis to form meanders.

A meander is a curve in a sinuous waterway or river. A meander forms when moving water in a stream erodes the outer banks and augments its valley, and the inner part of the waterway has less energy and deposits silt. A stream of any volume may accept a meandering course, on the other hand disintegrating silt from the outside of a curve and storing them within.

The process of meandering depends upon the following factors:

- 1. Discharge of the River:** When the discharge of a river is more its capacity to carry silt load is also more. When the water carries excessive load, meanders may be formed.
- 2. Sediment load in the River Water:** Composition of sediment load as well as its rate of movement affects the meandering process to a great extent.
- 3. Bed Slopes:** A change in the bed slope of the river also changes the meander pattern.

4. Bed and Bank Resistance to Erosion: Meanders are formed after cutting up of the banks. Obviously meandering process is affected by grain size, specific gravity, cohesion and roughness of the alluvium which is found in the bed and the banks. The reason for it is that the boundary resistance is characterized by these properties.

The protection of banks of a meandering river is done by providing structures like groynes on the concave face of the channel. They are usually provided in series for longer channel and singly for curved sections.

1.3. BACKGROUND

FLOW IN A CHANNEL BEND

Flow in a channel bend is more complex than in a straight channel. This is mainly due to the presence of secondary currents. Secondary currents are a characteristic feature of flow in open-channel bends. Besides the classical helical motion, a smaller and weaker counter-rotating circulation cell is often observed near the outer bank, which is mainly believed to play an important role in the bank erosion processes.

As flow enters to the bend channel, it is acted upon by the centrifugal forces which push it towards the outer bank of the channel. Since the magnitudes of bed velocities are lesser than those at the surface, hence surface velocities experience a greater centrifugal force, and therefore move faster towards the outer bank than bed velocities. When they reach the outer bank an increase in water elevation occurs due to a sudden decrease in velocity. This creates a radial pressure gradient, due to the water surface slope, which is equal to gravitational acceleration multiplied by the water surface slope. This pressure gradient is uniform over the flow depth at a specific point along the radius. As the flow near the bed experiences a smaller centrifugal force than at the surface, the radial pressure gradient eventually exceeds the centrifugal force (Fig. No.1), causing the water to deflect towards the inner bank at the bed. This process continues, and creates what is known as a helical flow pattern.

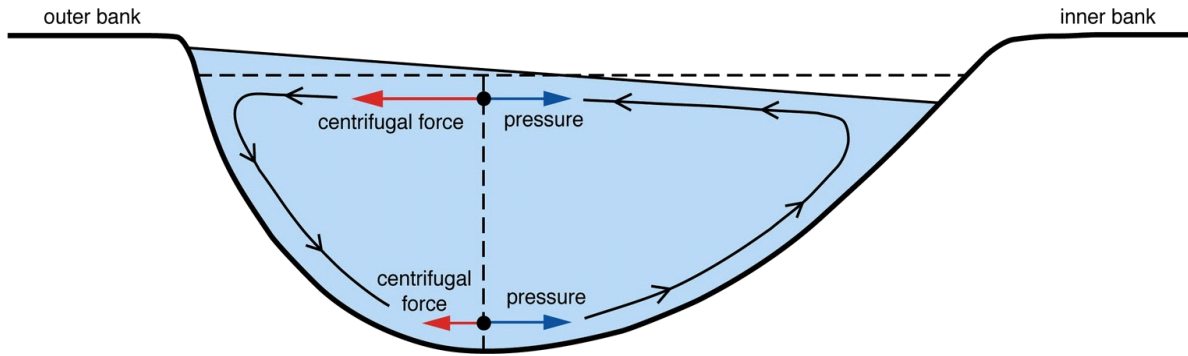


Fig. No.1 Helical flow in bend

Table 1-CHANNEL AND GROUYNE DESCRIPTION

REFERENCE	BEND DESCRIPTION	GROYNE CLASSIFICATION	GROYNE PERFORMANCE
Victoria Bend, Mississippi River (Jia et al. 2009)	Radius/Width= 1 to 3	Repelling and submerged	High scour around groynes, deposition upstream.
Jamuna River, Bangladesh (Mosselman et al. 2000)	Radius/Width= 2.7	Permeable, emerged	Outer bank erosion of 9 m, deposition at inner bank, outer bank stopped retreating.
Red Rock Bend, Mississippi River (WST 1999)	Radius/Width>3.5	Repelling	Large scour below 7 downstream weirs, less at 2 upstream weirs.

1.4. OBJECTIVES OF STUDY

- The objective of this study is to analyze the velocity flow patterns and shear stresses due to introduction of groyne in a channel bend at different positions.
- To investigate the effect of groyne installation on separation zone length behind it.
- To predict the most efficient position and size of the groyne for protecting the concave face of the river bend.

1.5. COMPUTATIONAL FLUID DYNAMICS

FLUENT is the CFD solver for complex flow ranging from incompressible to highly compressible flows. It provides multiple choices of solver option, combined with a convergence-enhancing multi-grid method. Because of its optimum solution efficiency and accuracy, it has been selected to simulate the groyne in this research. The FLUENT's parallel solver has the ability to use multiple processors that may be executing on the same computer, or on different computers in a network to decrease the computing time. This capability has been used in the present study using a dual core computer in order to reduce the simulation time and numerical efforts.

To prevent the river bank from erosion, groyne is placed on the concave face of the channel. And after searching for the relevant literature, the following dissertation was taken up.

1.6. RESEARCH STRATEGY

The simulation study for groyne placement in a river is done using computational fluid dynamic software, Ansys Fluent (v15) or using AUTO CAD (2015) for defining the channel geometry and then imported into Ansys, all other processes to get the required results will be done under the domain of this software.

The performance of groynes in channel bends has not always been documented. Some recent field studies, which document their performance, are listed in Table 1. Although this table is not exhaustive, it gives a general idea of groyne performance in the field.

With reference to the above rivers in table 1, the simulated channel section is designed with criteria of Mean Radius/Width=2.

The channel width is assumed a constant value of 20m, thus the mean radius is taken as 40m. The height of the channel section is taken as 8m.

The numerical simulations were taken for groyne of 6 different sizes, that is, 4m; 3.5m; 3m in length and 0.2 & 0.5m width. These sizes conform to the design criteria giving by the 'Indian Standard Code IS 8408:1994', which restricts the size of groyne to 1/5 times the channel width.

Three different velocities of 2m/s; 1.5m/s and 1m/s were taken for the numerical simulations to study the variation of velocity flow patterns and shear stress. Since in order to find the best size of groyne, analysis of dependent factors is done and then that efficient size is analyzed for different

positions and the best is decided among these after analysis of other dependent factors.

The primary aim of this project was to protect the concave face of the river bank and find the most efficient placement of the groyne in the bend channel.

1.7. RESEARCH CONSTRAINT

The observations taken in this study are not exhaustive in themselves and further analysis and iterations can be taken to find the best placement of groyne.

The software used for analysis Ansys Fluent (v15) also has some limitations-

- a) The channel boundary cannot be defined as non-rigid or movable hence extent of scouring on the banks and bed could not be estimated.
- b) The channel bed slope could not be defined as an input.
- c) Linear measurement like arc length could not be measured precisely and attribute of other software was needed for same.

1.8. ORGANISATION OF DISSERTATION

The report is subdivided into 6 chapters. Chapter 1 states the importance of the matter and objective of the study. Chapter 2 presents the review of the literature available on this topic. The methodology and numerical data involved in this dissertation work is discussed in Chapter 3. The results and the discussions are enlisted in Chapter 4. Finally in Chapter 5, conclusions and scope of future work are discussed.

CHAPTER 2

LITERATURE REVIEW

2.1. GROYNES

Groynes are the structures that are aimed at diverting the flow from the river embankment, commonly used in river engineering to prevent bank erosion and control the river from meandering. Depending upon the purpose, groynes can be used singly or in series.

Groynes are the embankment type structures, constructed to the transverse to the river flow, extending from the bank into the river. They are constructed, in order to protect the bank from which they are extended, by deflecting the current away from the bank. High velocities are usually found around groyne tip. Since in a channel bend the complexities of flow and the factors involved are numerous thus it is important to understand the factors which contribute the most and are critical for any further study.

2.2. SIGNIFICANCE AND WORKING OF GROYNES

Groynes serve additional functions such as improving channel navigability by deepening the river centerline; for training the river in a designated path; aiding in flood management and to maintain equilibrium of suspended and settled alluvium.

A groyne creates and maintains a wide area of sediment on its upstream side, and reduces erosion on the other. It is a physical barrier to stop sediment transport in the direction of longshore transport. This causes a build-up, which is often accompanied by accelerated erosion of the downstream beach, which receives little or no sand from longshore transport. Groynes add sediment to the beach by capturing downward drift. However, this can cause severe erosion on shorelines downstream from the groyne. So, it is necessary to place a correctly designed groyne, so that the amount of sediment it can hold will be limited and the excess sediment will be free to move on through the system.

2.3. SIGNIFICANCE OF POSITION OF GROYNES

Groynes mainly performs three functions, they deflect flow and secondary currents away from the river bank, they disrupt high velocity gradients in the near bank region, and they shift the boundary closer to the channel centerline. In this way they may provide a longer-term solution to mitigate

bank migration. The protection of banks of a meandering river, where curvature is high or to protect the bank is conventionally done by providing structures like groyne on the bank.

2.4. OBJECTIVES OF GROYNES

Main objectives of constructing a spur are-

- a. It trains the river along a desired course by attracting, deflecting or repelling the flow in a channel.
- b. Reduces the flow concentration at the point of attack by altering flow direction.
- c. Protects the bank by keeping the flow away from it.
- d. Dampens the flow and reduce the velocity due to energy dissipation in the eddy.
- e. Increases the depth of flow for navigation purpose by reducing width and aligning a wide and poorly defined channel into well-defined channel.
- f. Controls wild meandering and migration of a stream to a defined course.

2.5. TYPES OF GROUYNE

Groynes can be classified according to four different categories-

1. **Method and material of construction:** Method of construction refers to whether the groynes are permeable or impermeable. Permeable groynes allow water to flow through them and work best in rivers with high sediment loads. As they are not able to reduce water velocities as much as impermeable groynes, permeable groynes should be used in milder bends, or in rivers with lower flow rates. They may be constructed from piles, bamboo or timber. Impermeable groynes do not allow water to flow through and will cause the current to deflect. They are favorable for protecting banks in navigable channels where a high flow depth is desired in the channel center. They are normally constructed from rock or gabions.
2. **Submergence:** Groynes may be submerged or non-submerged under normal water conditions. Impermeable groynes typically experience high scour along their side walls when they are submerged, and thus are usually designed to be non-submerged. Permeable groynes work better under submerged conditions due to the smaller amount of local scour they induce.
3. **Effect on the stream flow:** This depends on the angle the groyne makes with the bank line, which classifies them as attracting, straight or deflecting. Attracting groynes point downstream, and attract flow towards themselves. They are less effective in bank protection,

as they do not redirect the flow towards the opposite bank. Straight groynes are perpendicular to the bank line, and change the direction of the flow, but do not repel the flow away from them. Deflecting groynes (also called repelling groynes) point upstream into the flow and repel the flow away from them by creating a high pressure zone on their upstream side and a low pressure one on their downstream side. The flow is therefore directed over them and towards the channel center.

4. **Appearance in plan view:** Groyne shapes include “straight”, “T-head”, “L-head”, “hockey”, “inverted hockey” and “wing” or “tail”. Straight groynes may have a rounded shape head to help deter scour. T-head groynes as the name suggests are in the shape of a “T” and are placed perpendicular to the bank. L-head and wing groynes are shaped to promote a larger deposit of sediment between them.

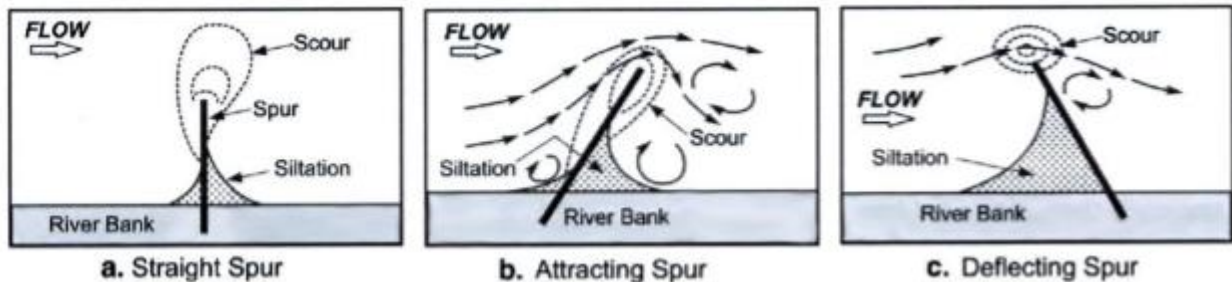


Fig. No.2 Classification of groynes by action on stream flow

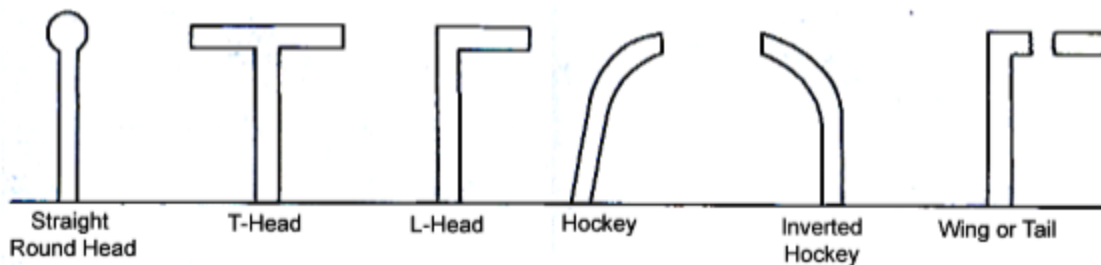


Fig. No.3 Classification of groynes by appearance in plan view

2.6. SEDIMENT TRANSPORT

In general, two modes of transport are studied:

- *Bed load:* particles sliding, rolling or saltating (making short jumps), but remaining essentially in contact with the bed.

- *Suspended load*: finer particles carried along in suspension by the turbulent fluid flow.

The combination of these two is called the *total load*.

- Dissolved load, $S_b + S_s = S$ (1)

Bed load transport refers to the particles or grains of sediment moved along the bed of a river which are all times wholly supported by the bed itself. In other words, bed load is bed material which moves by sliding and rolling, largely as a result of the shear stress exerted on the boundary by the flowing water. Mainly, bed load consists largely of the coarser fraction, the sand and gravel, of the sediment available to the river. Bed load transport in many rivers commonly does not occur or is negligible at low flow, but as flow increases, the shear stress at the boundary eventually will exceed the *threshold or critical conditions for bed particle movement* and bed load transport will become active.

Bed load transport typically moves a small amount of sediment relative to the total sediment load and generally is less important than the suspended-load component in the context of sediment budgets.

$$S_b = 8(\Delta g D^3)^{1/2} (\mu \theta - 0.047)^{3/2} \quad (2)$$

in which μ is a ripple factor, depending on sediment characteristics and the water depth.

θ is the Shields parameter: $\theta = u^2 / (\Delta g D)$. The Meyer-Peter-Müller formula is valid for $\mu \theta < 0.2$, $D > 0.4$ mm and $w_s / u_* > 1$.

Suspended-sediment transport refers to the particles or grains of sediment moved along a river within and wholly supported by the flow. In order for sediment grains to remain in suspension the upward-directed forces associated with turbulence in the flow must be strong enough to overcome the downward force of gravity acting on the grains. As physical reasoning implies, the suspended-sediment load consists largely of the finer fraction, the fine sand, silt and clay, of the sediment available to the river. Because turbulence is generated at the channel boundary and is most intense there, suspended sediment tends to have higher concentrations and involve coarser material near the boundary and both sediment size and concentration decline as we move up through the water column towards the surface of the flow.

$$S_s = \int_a^h uc dz \quad (3)$$

where u is the velocity and c is the sediment concentration.

$$6 > w_s/u^* > 2 \quad \text{bed load} \quad (4)$$

$$2 \geq w_s/u^* \geq 0.6 \quad \text{saltation} \quad (5)$$

$$0.6 > w_s/u^* \quad \text{suspension} \quad (6)$$

Where u^* is the shear velocity and w_s is the settling velocity.

$$W_s = \left(\frac{4}{3C_D} \Delta g D \right)^{1/2}, \text{ where } \Delta = \frac{\rho_s}{\rho} - 1 \quad (7)$$

where C_D is the drag coefficient dependent on the particle Reynolds number Re_p .

$$W_s = \frac{\Delta g D^2}{18\nu} \quad 1 < D \leq 100\mu m \quad (8)$$

$$W_s = \frac{10\nu}{D} \left(\sqrt{1 + \frac{0.01\Delta g D^3}{\nu^2}} - 1 \right) \quad 100 < D \leq 1000\mu m \quad (9)$$

$$W_s = 1.1\sqrt{\Delta g D} \quad D > 1000\mu \quad (10)$$

From this the dissolved load can be calculated.

2.7. STATUS OF RESEARCH WORK

Prasad Krishna S, Indulekha K.P, Balan.K, (2015)¹ analyzed the effects of placing of groynes at different angles from 45° to 135° & to find the most effective arrangement for minimizing the erosion of bank. In their study they created a undistorted model in a rectangular flume size 12.95m length, 1.2m width and 0.95m height in the hydraulics laboratory with pre-defined bed slope and side slope. Experiments were conducted in the river model, with & without the groynes, for a discharge of 0.33m³/s. Erosion/deposition patterns, velocity and flow depths were measured at different sections. He performed two experiments, firstly, single groyne placed at different angles and secondly multiple groynes, parallel and alternate arrangement. They concluded that the velocity and water level profiles indicate that groynes can be used for increasing centerline velocity and water levels in the upstream side for the purpose of navigation. Deposition is observed in the upstream side of the groyne may be due to the velocity reduction of the flow due to

groyne. More erosion was observed on opposite bank of groyne and erosion free zone was observed near the groyne and this length of erosion free zone changes on changing the angle of groyne installation. Maximum protection was obtained for an angle of 135° in single groyne experiment. In multiple groynes, alternate arrangement showed more increase in the water levels & velocities compared to parallel arrangement. But the erosion percentage was less for parallel arrangement. There was no erosion between the groyne fields in both the arrangements.

J.Yazdi & H. Sarkardeh(1989)², simulated the flow patterns around a single spur dike with free surface flow using a numerical model known as fluent. The model was used to predict flow near the structure where the dimensional flow was dominant. In this research work, both a structured and an unstructured mesh were used & density of the mesh spacing near the walls was made greater than the other mesh. Comparison of free surface and velocities of 3D model is done. The reattachment length for various conditions was measured using numerical results, flow patterns and bed-shear stress distribution was presented for repelling, attracting & vertical spurs together. The $k-\omega$ turbulence model with the VOF method was used to simulate fully 3D flows. The study showed that length and width of the recirculation zone for various angles of spur dike are approximately constant. Also varying the discharge has little effect on the reattachment length, but changing the length of the spur dike has considerable effects on the dimensions of recirculation zone. The maximum bed-shear stress was observed in vertical spur dike rather than for the spur dikes oriented upstream or downstream. Also the effect of flow discharge and the length and angle of spur dikes upon the bed-shear stress distribution was evaluated.

Shamloo Hamid and Pirzadeh Bahareh³, established the subcritical flow pattern around an indirect groyne in six different angle of installation and 3D simulations in Fluent software have been applied to investigate the effect of angle of groyne installation on separation zone length behind it. In all their cases the groyne length and inlet flow depth were constant and the bed slope of the channel was zero. Their experimental set-up was 40 m long open channel flume with a rectangular cross-section with 2 m in width and 0.65 m in depth. The groyne length taken was 30cm. In their study flow pattern changes induced by a single groyne in a rectangular open channel were numerically simulated using a three-dimensional Finite Volume CFD model. The numerical model was simulated with groyne at different angles. Comparison of the velocity value on the groyne nose, the separation length downstream of the groyne, and the incidence angles with the

physical model measurements completed by Yeo et al. (2005) was done. The separation length provides good knowledge of the groyne installation interval. It showed that, it is about 12 times the impermeable groyne with 30 cm length. Their results indicate that with an increase in groyne installation angle, the difference between velocity values in the main flow region and the return flow area increases, and also the location of the return flow area centre shifts away from the channel sidewall.

Suharjoko, Mohammad Bisri, and Muhammad Ruslin Anwar(2001)⁴, described for a good placement of groyne on the river bend and the analyzed the behavior of flow current that occurs. The purpose of Case Research was carried out by the flow simulation repeatedly on various cases groyne placement with several alternative flows. Simulations are done using mathematical modeling approach by finite difference method. The research was done for the case of groyne placement on the river bend of radius 30m and 40m. 90 times simulation was done for different length of groynes at different velocities. The three variations of the position were taken i.e. Position 1 on the upstream arc bends, Position 2 in 1/4th upstream arc curves and Position 3 in the middle of the arc bends. The result described according to the case of groyne placement to the river having radius bend $R=40$ m, the groyne in 1/4 upstream arc curves bend give a better effect to control the flow than another groyne placement. And for the case of groyne placement to the river having radius bend $R=30$ m, the groyne in upstream arc curves bend give a better effect to control the flow than another groyne placement. From the Length of Groyne Considerations, analysis of the relationship between long-groyne factors (L/B) with the protection factor (D/B) be occurred that the length factor (P/B) is equivalent to 1/5 of the river width had indicated to give a better effect to protection factor (D/B) than another groyne length factors be purposed.

Mohammad Vaghefi; Masoud Ghodsian; and Seyed Ali Akbar Salehi Neyshabouri, (2016)⁵, studied the topography of the bed around a T-shaped unsubmerged spur dike located in a 90° bend and geometry of the scour hole formed. The experiments were carried out in a channel with a 90° bend. Uniform sediments having an average diameter of 1.28mm were used under clear-water scour conditions. The effects of parameters like the length of a spur dike, the location of a spur dike in the bend, the radius of bend, the wing length of a spur dike and flow intensity on the scour around a T-shaped spur dike were investigated. A new equation for scour parameters at a T-shaped

spur dike is developed. Experiments for this investigation were carried out in the laboratory with the main channel consisted of a 7.1 m long upstream and a 5.2 m long downstream straight reach.

The main results of their experimental study are: Two scour holes are formed because of a T-shaped spur dike: one at the nose of the spur dike and the other at the downstream side of the spur dike. When the spur dike is located at sections 30 or 45°, the height of the sediment deposition ridge is higher than when the spur dike is located at sections 60 or 75°. Any change in the position of the spur dike toward the downstream portion of the bend increases the scour depth. The location of maximum scour depth is at the upstream side of the spur dike and at the distance of 10–20% of the spur dike length. By increasing the radius of the bend, the maximum scour depth decreases. Because the research study was conducted in a fixed bank rectangular channel, additional work can be done to confirm the presented experiments for a movable channel bank.

Mohammad Vaghefi, Masoud Ghodsian, and Maryam Akbari, (2016)⁶, investigated the flow field around a T-shaped spur dike located in a 90° bend experimentally. The three-dimensional Acoustic Doppler Velocimeter (ADV) was used for measuring the flow field. The comparison of the three dimensional components of velocity was made in different sections of the bend and the differences of the flow pattern along the bend was analyzed. The observations showed the significant effect of the spur dike on the secondary flow patterns. Some horizontal vortices with a counter-clock-wise direction were also observed in the up and down stream of the spur dike near the outer bank of the bend. The reverse flows and vortices in the up and down stream of the spur dike, the changes in the secondary flow and vorticity were also investigated in their study. They conducted an experimental study on how changes in Froude Number, length of wing and web of T-shaped spur dike located in a 75° position affect flow pattern in a 90° bend. They proved that as the length of the spur dike increases, the length of separation zone and the formed vortex in the zone also increases. The main channel consisted of a 7.1m long upstream and a 5.2m long downstream straight reaches. A 90° channel bend was located between the two straight reaches. The channel was of rectangular cross section 0.6m width; 0.7m height with 2.5m radius of bend to centerline. The spur dike was made of Plexiglas (1 cm thick) T shaped in plan. The length of spur dike and its wing was 9 cm. The spur dike was located at 75° cross section of the bend. In section 30° of the bend, secondary flow is formed near the inner bank and in the upper layers of the flow. The secondary flow continues to exist up to section 65° while wavering and becoming weak. In sections close to

the spur dike wing, longitudinal components of velocities at first and second layers near the wing are higher. By moving to the downstream direction of the bend, longitudinal components of velocities at the upper and middle layers grow. Near the outer bank of bend, the magnitude of velocity is less. The variations of strength of secondary flow and vorticity follow the same trend along the bend.

Ruther and Olsen (2005); Khosronejad et al. (2007)⁷, concluded that the flow in a curved channel is subjected to a helical flow induced by centrifugal forces, which leads to high shear stresses along the outer bank. Groynes attempt to disrupt this helical pattern, and shift high velocities back to the channel centre line, thereby lowering the velocity gradient along the outer bank. Kinzli and Thornton (2009) demonstrated the ability of partially submerged weirs to do this in a series of 72 tests conducted in a rigid bed laboratory meander flume. The weirs varied in length, angle, and spacing ratio. In all the cases it was found that the maximum velocity within the recirculation zone immediately downstream of the weir was always lower than the maximum main channel centerline velocity just upstream of the weir. Abad (2008) showed that for emergent groynes the core of high stream wise velocities in the channel bend stayed inwards of the groyne tip.

Majid Fazli, Masoud Ghodsian, and Seyed Ali Akbar Salehi Neyshabouri, (2008)⁸, presented the experiments on flow field and scour around a spur dike in a 90° channel bend. Experiments were conducted for different lengths and different locations of spur dikes at the bend with different values of discharge. The three dimensional flow fields around a spur dike were investigated. The maximum depth of scour was correlated to the Froude numbers, lengths and the locations of spur dike in the bend. Experiments for this investigation were carried out at the Hydraulic Laboratory with the main channel consisted of a 7.1m long upstream and a 5.2m long downstream straight reaches. A channel bend of 90° was located between the two straight reaches. The channel was of rectangular cross section 0.6 m width, 0.7m height with 2.5m centerline radius of bend. Experiments were conducted to study scour and flow pattern around a spur dike located in a 90° channel bend. The attributes of the scour hole have been appeared to be influenced by the location of spur dike in the bend, Froude number and length of spur dike. Also the characteristics of flow pattern have been shown to be affected by the location of spur dike. It was found that by increasing the distance of spur dike location from beginning of bend, the stagnation zone before

spur dike increases, while standing eddy zone after spur dike decreases. A circulating flow observed in the cross sections before and after the spur dike with direction from inner bank to outer bank. After the spur dike a vortex up flow forms near the outer bank. The dimension of the scour depth when spur dike is located in the first half of the bend (before apex of bend) is smaller than when spur dike is located in the second half of the bend. Bed topography in the bend is affected by the location of spur dike in the bend. When the spur dike is located in the second half of the bend, deposition is occurred near the outer bank at the exit of the bend. When spur dike is located in the first half of the bend erosion occurred in this region. Redirection of water by the spur dike cause a narrow zone of debasement in the channel from upstream stagnation zone up to downstream of standing eddy zone. They also concluded that Froude number is an important parameter and has a direct relation to maximum relative scour depth and height of point bar. By the increment in Froude number these parameters also increases. By increasing the length of spur dike, the scour depth increases.

A. R. Masjedi and H. Moradi, (2008)⁹, one of the most important subjects in spur dike design is investigation of scouring and determining the depth of scouring in the head land of spur dike. They concluded that one of the influencing parameters on the depth of scouring around spur dikes is the position of spur dike in the bend. Tests in a laboratory flume with 180° bend with ratio R/B=4.7 of Plax glass material is done for investigating the effect of position of installation of groyne in the bend. In their research, spur dike was installed in the laboratory flume with positions 30,60,90,120,150 and 160 degrees with discharges 24 Lit/s and fixed depth 13 cm. Phenomenon of scouring around spur dike in pure water was investigated. For examination of impact of discharge value and spur dike position on the scouring depth in the bending all the while, changes of dz/L versus spur dike position in the bend is plotted for three different discharge values. The graph indicates that maximum scouring depth around the spur dike has the direct relation with spur dike position and discharge values and it increases by increasing resting angle of spur dike or increasing discharge values.

Ahmed Hassan Safi, Mohammad Mahdi Hasan, and Norio Tanaka, (2009)¹⁰, studied the influences of floodplain impermeable groynes on flow structure, velocity, and water depth around the groyne experimentally. A wooden symmetrical compound channel was used for the study. The flume is 0.50 m in depth, 0.50 m in width, and 15.0 m in length. Groyne models with three

different relative lengths 0.5, 0.75 and 1.0 were used on one floodplain with single and series arrangements. The conclusions drawn from the experiments was that the flow structure, velocity, and water depth mainly depend on the groyne type, relative length, and relative distance between two groynes in series arrangements. Utilizing an impermeable groyne with an expansive relative length on a river floodplain creates flow eddies and separation zones downstream of the groyne and in the upper area of the principle channel that may prompt floodplain erosion. The velocity in the main channel upper region decreases, while in the middle and lower regions of the main channel it increases. The velocity on the other floodplain also increases. In cases of a single groyne when Relative length = 0.5, 0.75, and 1.0, the negative velocities reached -20%, -30%, and -55% of the original velocity, respectively. Those negative velocities were substituted by increasing the flow velocity in the main channel and on the opposite floodplain. The increase could reach 1.4, 1.6, and 1.85 times the original velocity in the main channel, and 1.75, 2.25, 2.75 times the original ones on the other floodplain. The effective distance between two symmetrical groyne on one side of the floodplain is from 3 to 4 times the groyne length. River levee and embankment failures can occur if the protection works against the scouring process are weak, and the river can easily change its course and centerline. To relieve those impacts, the groyne length ought to be not as much as a large portion of the floodplain width.

CHAPTER 3

METHODOLOGY

3.1. INTRODUCTION

Simulation Studies were conducted on hypothetical channel for assessment of effect of placement of groyne on separation zone length behind it and consequent meandering of the banks of river.

The use of computational fluid dynamics software is very much helpful in solving partial differential equations based on conservation principles.

The main purpose of the simulation described below is to get the optimum number of observations for further analysis to be done. Though, the observations taken here are not exhaustive in any respect. As to find the best placement of the groyne, increase in the data would also increase the accuracy of the results. So, the properties considered for the purpose of simulations are as follows.

3.2. DESCRIPTION OF HYPOTHETICAL CHANNEL MODEL

3.2.1. CHANNEL CHARACTERISTICS

For the following study, the channel had a rectangular section for the straight reaches and a curvature for the bend sections.

The straight reaches at the beginning of the section and the end of curvature is as follows-.

- a) Length=20m
- b) Width =20m (constant for the whole section)
- c) Height=8m

The mean radius of curvature of the bend is taken as 40m.

The dimensions used for simulation are with reference to a research paper.

The channel boundary and bottom are assumed to be made up of a material that is non-scouring i.e. the boundary conditions of the channel is non mobile. This means that the effect of alluvium is not considered in flow patterns or shear stress in this study.

3.2.2. GROUYNE CHARACTERISTICS

The groyne used in the study is assumed to be made up of gypsum ($\text{CaSO}_4 \cdot 2\text{H}_2\text{O}$) with material characteristics as follows. It should be noted that since scouring effects are not considered in this study thus by using different groyne material no significant difference in results is observed.

The groyne used is non-permeable in nature and work as non-submerged groyne at every section of the channel.

Groyne used is of rectangular correction with lengths of 4m, 3.5m and 3m were used for making observations. The width of the groyne taken is 0.2m and 0.5m.

Since the primary objective of this simulation study is to protect the concave face of the bend, so, only the groyne is provided at this face of the bend at different positions.

3.3. POSITION OF GROUYNE FOR STUDY

In this study, groyne placement was considered at three different sections along the channel bend. The position for the initial section for the placement was decided by taking into observation the flow velocities in a channel without any groyne that is without any protection.

Position A-at upstream arc of the bend

Position B-at $1/4^{\text{th}}$ upstream arc

Position C-at middle of the arc bend

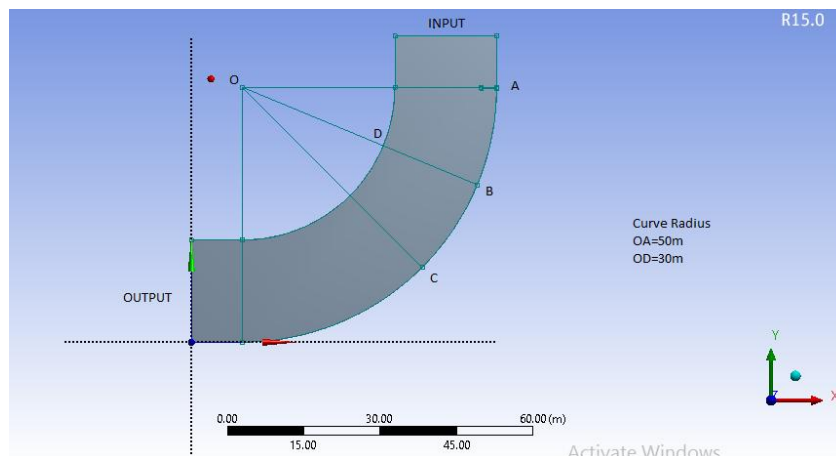


Fig. No. 4 Orientation of groyne placement

$$OA=R_1=50\text{m}$$

OD=R₂=30m

Below are the different positions of groyne placement at the concave face of the bend

Table 2-Position of different groyne at concave face

	a	b	C	d
POSITION(in degrees with respect to meridian “OA”)	$\theta=15^\circ$	$\theta=30^\circ$	$\theta=45^\circ$	$\theta=60^\circ$

3.4. INPUT VARIABLES

Three different velocities of 2m/s; 1.5m/s; 1m/s are used in this study for the results. These input velocities are average velocities through which the computations are initialized.

The lengths of groyne used for study are 4m, 3.5m, 3m. These groyne are non permeable in nature. The groyne used on the concave bank of channel is repelling in nature and thus they are pointed upstream.

3.5. MEASUREMENTS

In order to determine the factors which determine the behavior of flow pattern due to a groyne certain basic measurements are needed.

3.5.1 PROTECTED LENGTH

It is the length of the concave side of the section that is protected due to the introduction of the groyne. This length varies with the size of the groyne, their placement and initial velocity of flow. The protected length of the convex face is not taken into consideration as before the introduction of groyne no protection was needed on this face. So, only protected length is measured on the concave face of the bend.

3.5.2 VELOCITY

There are namely three velocities that are either given as input or measured-

- a) Approach Velocity (V_{app})-this is the input velocity that is given to initialize the simulation.
- b) Tip Velocity (V_{tip})-this is the velocity measured near the tip of the groyne

- c) Maximum Velocity (V_{\max})-this is the absolute or global maximum velocity in the channel.

3.5.3 SHEAR STRESS

The shear stress that is taken into consideration or assumed as an important factor for analysis is the maximum bed shear stress. This stress was found to be maximum in all the cases near the groyne. It is represented by the symbol Γ_{\max} .

To know the increase in stress due to introduction of groyne in the channel, initial bed shear stress was also measured and it was measured at the centre line on the channel. It is represented by the symbol Γ_0 .

3.6. COMPUTATIONAL FLUID DYNAMICS AND GOVERNING EQUATIONS

It is the qualitative and quantitative prediction of fluid flows. CFD uses numerical methods containing a set of governing equations and algorithms to solve and analyze problems that involve such fluid flows. ANSYS FLUENT is a CFD software that works on the principle of Finite Volume Method (FVM) where the domain are divided into finite set of control volumes. The fundamental basis of almost all CFD problems is the Navier–Stokes equations, which define many single-phase fluid flows. In the simulation, the equations are solved iteratively as a steady state or transient.

The governing equations in computational fluid dynamics are

- Conservation of Mass

$$\frac{\partial \rho}{\partial \tau} + \frac{\partial \rho U_i}{\partial x_i} = 0 \quad (11)$$

- Conservation of momentum

$$\frac{\partial \rho U_i}{\partial \tau} + \frac{\partial \rho U_j U_i}{\partial x_j} = \frac{\partial}{\partial x_j} \left(\mu \frac{\partial U_i}{\partial x_j} - \rho u_i u_j \right) - \frac{\partial P}{\partial x_i} + S_{ui} \quad (12)$$

- Continuity equation

$$\frac{\partial \rho}{\partial t} + \nabla \cdot (\rho V) = 0 \quad (13)$$

- Energy equation

$$\rho \frac{D}{Dt} \left(e + \frac{V^2}{2} \right) = \rho q + \frac{\partial}{\partial x} \left(k \frac{\partial T}{\partial x} \right) + \frac{\partial}{\partial y} \left(k \frac{\partial T}{\partial y} \right) + \frac{\partial}{\partial z} \left(k \frac{\partial T}{\partial z} \right) - \frac{\partial (up)}{\partial x} - \frac{\partial (vp)}{\partial y} - \frac{\partial (wp)}{\partial z} +$$

$$\frac{\partial(u\tau_{xx})}{\partial x} + \frac{\partial(u\tau_{yx})}{\partial y} + \frac{\partial(u\tau_{zx})}{\partial z} + \frac{\partial(v\tau_{xy})}{\partial x} + \frac{\partial(v\tau_{yy})}{\partial y} + \frac{\partial(v\tau_{zy})}{\partial z} + \frac{\partial(w\tau_{xz})}{\partial x} + \frac{\partial(w\tau_{yz})}{\partial y} + \frac{\partial(w\tau_{zz})}{\partial z} + \rho f \cdot V \quad (14)$$

3.7. SOFTWARE INPUT

The computational fluid dynamic software used for carrying out this study is Ansys Fluent (v15). This software gives us the required results by simulating flow patterns in the given channel using a predefined mathematical model.

This software consists of 4 basic parts which together give the required results for a certain study. These, are enumerated below, are software prerequisites and are essential for every case of observation to be made.

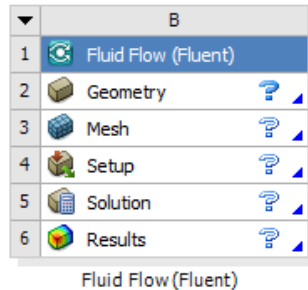


Fig. No. 5 Dialog box showing basic components of Ansys Fluent.

3.7.1. GEOMETRY

This is the part of the software that is used to define the channel geometry and its cross section. It is named as ‘Design Modular’ in Fluent.

There are essentially 2 ways to define the geometry of the required channel-

a) To design/draw the geometry using the tools in design modular. The section is firstly drawn in a 2-Dimensional plane of either X-Y, Y-Z or Z-X.in order to get a 3-Dimensional structure the above plane is given height or width in the direction perpendicular to the plane. Ex- for a section drawn on X-Y plane the channel is given width or height in the Z direction to obtain a 3-D structure. This is done in Ansys Fluent using Design Modular inbuilt tools like ‘extrude’, ‘sweep’.

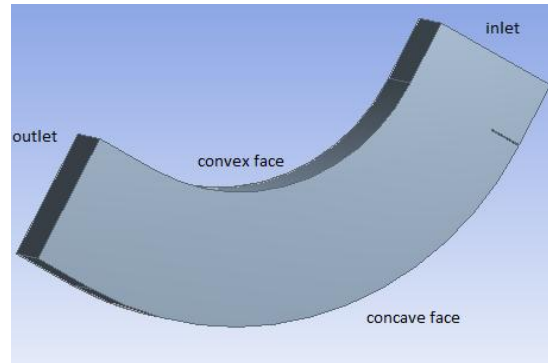


Fig. No. 6 Channel Geometry as it looks in Design Modular of Ansys Fluent

b) The required section of channel can also be drawn in other Computer Aided Design (CAD) software like Auto CAD2016. The supported file of this geometry is then imported into the Design Modular.

3.7.2. MESHING

Meshing is a fundamental part of the computer-aided engineering simulation process. The mesh influences the exactness, convergence and speed of the solution. Furthermore, the time it takes to create and mesh a model is often a significant portion of the time it takes to get results from a solution. Therefore, the better and more automated the meshing, the better the solution.

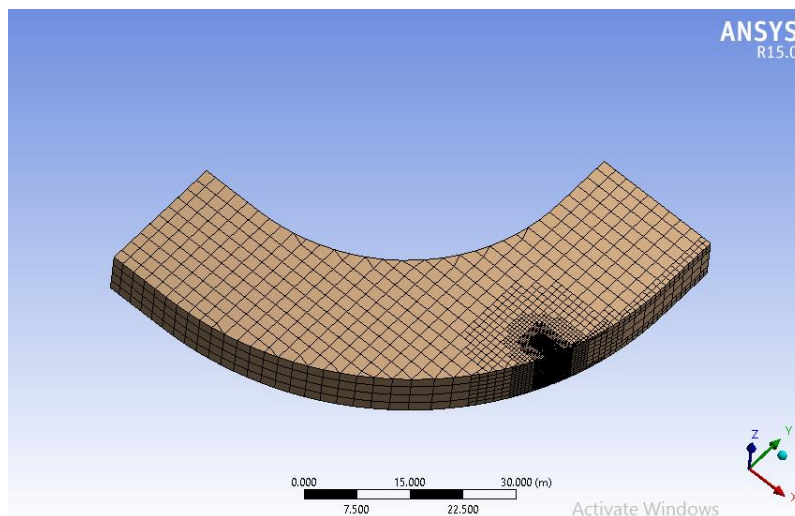


Fig. No. 7 Meshing by Cut Cell Assembly method with relevance to proximity and curvature.

For the study undertaken the flowing meshing was used to get appropriate results-

Table 3-Meshing Components and the assigned values/method for study.

COMPONENTS	Size or Function	Relevance center	Smoothing	Min. size	Assembly Method
VALUES/METHODS	Proximity and Curvature	Coarse	Medium	0.17888m	Cut cell

It is also necessary to define the channel components, like convex face, concave face, inlet, outlet, channel bottom, groyne, and top of channel. These are also defined for the next step of setup where these are read into file so that characteristics of each of these components can be defined. Like their material and their functioning in the simulation process.

3.7.3. SETUP

It is the step in Ansys Fluent where the mathematical model to be used, definition of components of channel like material and their type, is done. The values needed to initialize the solution i.e. the input velocity is provided in this step.

For the following study the mathematical model that was chosen for all the observation was ‘K-EPSILON (2eqn)’, this model gave moderately conservative results. The predefined values for this type of model are-

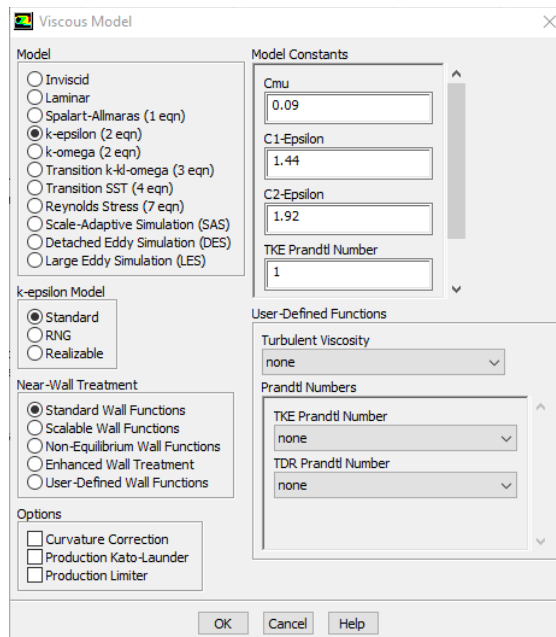


Fig. No. 8 Definition of mathematical model used, k-epsilon.

This model is used in CFD to simulate mean flow characteristics for turbulent flow conditions. It is a two equation model which gives a general description of turbulence by means of two transport equations (PDEs). The original impetus for the K-epsilon model was to improve the mixing-length model, as well as to find an alternative to algebraically prescribing turbulent length scales in moderate to high complexity flows. This model was applied assuming a steady state condition and not transient. Gravity is defined as a constant value of 9.81m/s^2 in the $-ve$ Y direction.

The boundary condition defined for the channel components is as follows-

Table 4- Boundary Condition for each case of observation.

Channel components	INLET	OUTLET	GROYNE	TOP	BOTTOM	BOUNDARY
Definition	Velocity inlet	Outflow	Wall	Symmetry	Wall	Wall

Three different velocities of 2m/s; 1.5m/s; 1m/s are used in this study for the results as a boundary condition from the inlet. These input velocities are average velocities through which the computations are initialized.

3.7.4. SOLUTION

This is step in which the solution methods for different computations are defined and also the monitors for control. The solution is initialized with values from ‘INLET’ in all the observation under this study. It is necessary to initialize a solution before any calculation on the input raw data can be done.

Table 5-Solution Methods used in this study.

Component	Pressure	Momentum	Turbulent kinetic energy	Turbulent dissipation rate	Gradient	Pressure-Velocity coupling
Method	Standard	Second order upwind	Second order upwind	Second order upwind	Least square cell based	Simple

Second order upwind scheme is the most stable discretization scheme and is used because it uses the values upstream to evaluate the property on the boundaries of the cell and then use them to compute the value at the center of the cell. As it is an "upstream" value, it takes into account the

flow direction. This is more accurate than first order.

For the steady state computations the number of iterations for different cases varied, as in each case the solution converged at different iterations. Reporting interval that is the interval after which solution of each set are displayed can be varied accordingly. These are complex calculations and thus it is recommended to define the number of system cores at the beginning of this step to accommodate the solutions easily, without any load on the workstation.

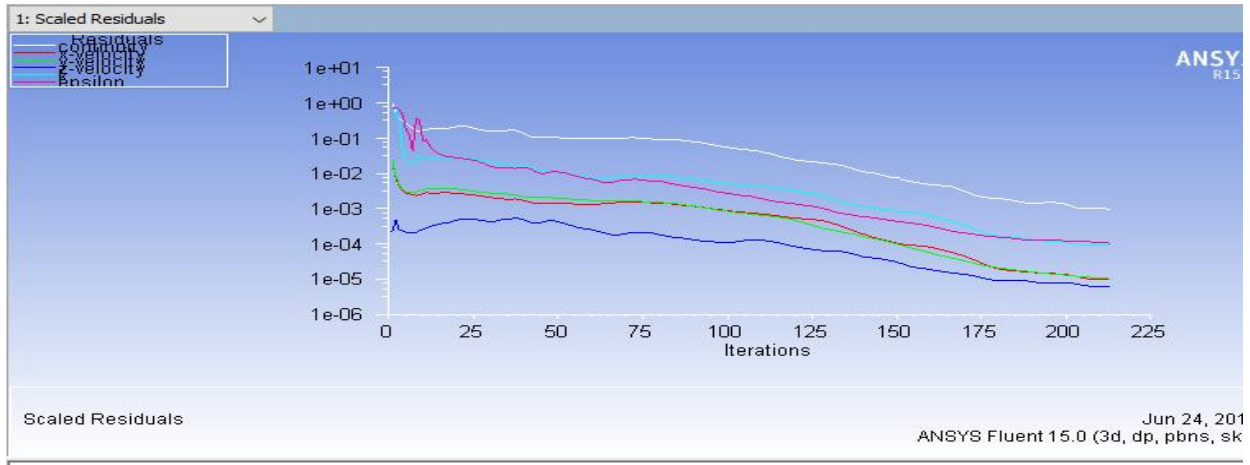


Fig. No. 9 One of the cases of this study where the solution converged at 213th iteration

CHAPTER 4

RESULTS AND DISCUSSION

4.1. INTRODUCTION

This chapter contains the result obtained from the Ansys Fluent. Different cases were run for groyne of different size, position and approach velocity.

The following table contains the values of tip velocity obtained from the Fluent software. The variation of this velocity around the groyne in the vertical direction is not linear.

Here V_{app} = Velocity of approach to groyne in m/s, V_{tip} = tip velocity at the groyne obtained numerically in m/s, τ_{max} = maximum shear stress near the groyne in Pascal, τ_o =initial shear stress measured at centre line in Pascal, D = protection length in m, B =width of channel in m, L =length of groyne in m.

NOTE-All the above observations are pertaining to the zone near the repelling groyne, since the aim of this study is to protect the concave face of the bend.

4.2. SOFTWARE OUTPUT.

The following table gives the values of tip velocity, maximum velocity, maximum shear stress, initial shear stress and protected length.

Table 6-For position A (UPSTREAM ARC)

GROYNE	Length of groyne (m)	Width of groyne (m)	Approach velocity V_{app} (m/s)	Tip velocity V_{tip} (m/s) (Coordinates of tip)	Maximum velocity V_{max} (m/s)	V_{tip}/V_{app}
1a	3	0.2	1	1.562 (52.4,45.4,3.45)	1.776	1.562
1b	3	0.5	1	1.228 (56.9,50.1,6.91)	1.771	1.228
1c	3.5	0.2	1	1.262 (56.57,50.15,6.76)	1.904	1.262
1d	3.5	0.5	1	1.61 (56.45,50.06,7.602)	1.902	1.61
1e	4	0.2	1	1.27 (56.11,50.29,6.56)	2.009	1.27
1f	4	0.5	1	1.57 (55.74,50.17,5.31)	2.017	1.57
2a	3	0.2	1.5	1.37 (57.04,50.04,7.58)	2.656	0.9133
2b	3	0.5	1.5	0.612 (57.06,50.03,2.58)	2.734	0.408
2c	3.5	0.2	1.5	0.3827 (56.7,49.46,4.308)	2.897	0.2551
2d	3.5	0.5	1.5	2.69 (54.98,50.07,7.86)	2.844	1.7933
2e	4	0.2	1.5	0.355 (56.49,49.7,4.74)	3.021	0.2366
2f	4	0.5	1.5	1.539 (55.66,50.23,4.39)	3.0228	1.026
3a	3	0.2	2	1.835 (57.03,50.05,7.89)	3.673	0.9175
3b	3	0.5	2	0.572 (56.91,50,0.514)	3.683	0.286
3c	3.5	0.2	2	0.586 (56.55,50.03,7.645)	3.837	0.293
3d	3.5	0.5	2	2.481 (56.608,50.1,7.55)	3.872	1.2405
3e	4	0.2	2	0.736 (55.96,50,7.92)	4.021	0.368
3f	4	0.5	2	1.515 (55.91,50.14,7.54)	3.975	0.7575

Table 7-For position B (1/4th UPSTREAM ARC)

GROYNE	Length of groyne (m)	Width of groyne (m)	Approach velocity V_{app} (m/s)	Tip velocity V_{tip} (m/s) (Coordinates of tip)	Maximum velocity V_{max} (m/s)	V_{tip}/V_{app}
1a	3	0.2	1	1.0923 (53.1382,31.05,6.682)	1.5021	1.0923
1b	3	0.5	1	0.1610 (53.0614,30.94,5.045)	1.494	0.161
1c	3.5	0.2	1	1.083 (52.6047,31.63,4.726)	1.5833	1.083
1d	3.5	0.5	1	0.171 (52.8215,30.64,6.52)	1.6181	0.171
1e	4	0.2	1	0.198 (52.13,30.7,2.2)	1.6618	0.198
1f	4	0.5	1	0.2342 (52.35,31.2847,7.654)	1.666	0.2342
2a	3	0.2	1.5	1.2798 (53.1,30.95,5.931)	2.2739	0.8532
2b	3	0.5	1.5	0.89 (53.3712,31.29,7.713)	2.2642	0.5933
2c	3.5	0.2	1.5	0.72 (52.724,31.32,7.69)	2.4043	0.48
2d	3.5	0.5	1.5	0.70 (52.732,31.377,7.3911)	2.4397	0.4666
2e	4	0.2	1.5	1.83 (51.96,31.11,6.967)	2.5247	1.22
2f	4	0.5	1.5	1.327 (52.48,31.372,7.011)	2.5314	0.8846
3a	3	0.2	2	2.219 (52.93,31.1,5.75)	3.0635	1.1095
3b	3	0.5	2	1.81 (53.252,31.38,4.78)	3.0426	0.905
3c	3.5	0.2	2	2.149 (52.76,31.012,7.854)	3.2339	1.0745
3d	3.5	0.5	2	2.017 (52.813,31.33,7.641)	3.2364	1.0085
3e	4	0.2	2	2.368 (51.682,31.316,5.3035)	3.3723	1.184
3f	4	0.5	2	2.427 (52.074,31.433,6.506)	3.3802	1.2135

Table 8-For position C (1/2 UPSTREAM ARC)

GROYNE	Length of groyne (m)	Width of groyne (m)	Approach velocity V_{app} (m/s)	Tip velocity V_{tip} (m/s) (Coordinates of tip)	Maximum velocity V_{max} (m/s)	V_{tip}/V_{app}
1a	3	0.2	1	1.0588 (42.344,15,6.625)	1.2935	1.0588
1b	3	0.5	1	1.058 (42.272,15.47,5.826)	1.2996	1.058
1c	3.5	0.2	1	1.074 (41.945,14.99,7.123)	1.3301	1.074
1d	3.5	0.5	1	1.07 (42.29,15.22,7.189)	1.3326	1.07
1e	4	0.2	1	1.116 (41.297,15.1,6.941)	1.655	1.116
1f	4	0.5	1	1.120 (41.296,15.48,4.39)	1.3751	1.12
2a	3	0.2	1.5	1.564 (41.69,15.56,3.86)	1.941	1.0426
2b	3	0.5	1.5	1.4947 (42.05,16.552,1.390)	1.9515	0.9964
2c	3.5	0.2	1.5	1.592 (42.002,14.94,7.776)	1.9955	1.0613
2d	3.5	0.5	1.5	1.5813 (41.97,15.705,2.1665)	2.0007	1.0542
2e	4	0.2	1.5	1.616 (41.484,14.928,7.733)	2.0492	1.0773
2f	4	0.5	1.5	1.5066 (41.723,15.23,7.022)	2.0699	1.0044
3a	3	0.2	2	2.114 (42.079,15.137,7.179)	2.590	1.057
3b	3	0.5	2	1.951 (42.768,15.262,7.575)	2.6048	0.9755
3c	3.5	0.2	2	2.079 (41.994,14.921,7.200)	2.6637	1.0395
3d	3.5	0.5	2	2.157 (41.74,15.632,4.521)	2.6747	1.0785
3e	4	0.2	2	2.2281 (41.372,15.029,6.882)	2.736	1.11405
3f	4	0.5	2	2.187 (41.646,15.339,7.155)	2.7670	1.0935

By examining the output data, conclusions made are that on increasing the groyne size and approach velocity, the maximum velocity also increases in all the positions of groyne.

Table 9-For position A (UPSTREAM ARC)

GROYNE	Length of groyne (m)	Width of groyne (m)	Approach velocity V_{app} (m/s)	Max. shear stress, Γ_{max} (Pa)	Initial shear stress, Γ_o (Pa)
1a	3	0.2	1	16.7104	1.259
1b	3	0.5	1	16.7104	1.259
1c	3.5	0.2	1	19.117	1.259
1d	3.5	0.5	1	16.7104	1.259
1e	4	0.2	1	16.7104	1.259
1f	4	0.5	1	16.7104	1.259
2a	3	0.2	1.5	16.7104	2.702
2b	3	0.5	1.5	16.7104	2.702
2c	3.5	0.2	1.5	19.1117	2.702
2d	3.5	0.5	1.5	16.7104	2.702
2e	4	0.2	1.5	16.7104	2.702
2f	4	0.5	1.5	16.7104	2.702
3a	3	0.2	2	22.724	4.6429
3b	3	0.5	2	17.2105	4.6429
3c	3.5	0.2	2	24.148	4.6429
3d	3.5	0.5	2	18.508	4.6429
3e	4	0.2	2	25.447	4.6429
3f	4	0.5	2	20.0193	4.6429

Table 10-For position B (1/4th UPSTREAM ARC)

GROYNE	Length of groyne (m)	Width of groyne (m)	Approach velocity V_{app} (m/s)	Max. shear stress, Γ_{max} (Pa)	Initial shear stress, Γ_o (Pa)
1a	3	0.2	1	2.825	1.259
1b	3	0.5	1	2.6953	1.259
1c	3.5	0.2	1	3.106	1.259
1d	3.5	0.5	1	2.8237	1.259
1e	4	0.2	1	3.2845	1.259
1f	4	0.5	1	3.0243	1.259
2a	3	0.2	1.5	6.0847	2.702
2b	3	0.5	1.5	5.7094	2.702
2c	3.5	0.2	1.5	6.631	2.702
2d	3.5	0.5	1.5	4.8593	2.702
2e	4	0.2	1.5	7.029	2.702
2f	4	0.5	1.5	6.402	2.702
3a	3	0.2	2	10.369	4.6429
3b	3	0.5	2	9.7552	4.6429
3c	3.5	0.2	2	11.3542	4.6429
3d	3.5	0.5	2	10.338	4.6429
3e	4	0.2	2	12.1038	4.6429
3f	4	0.5	2	11.2299	4.6429

Table 11-For position C (1/2 UPSTREAM ARC)

GROYNE	Length of groyne (m)	Width of groyne (m)	Approach velocity V_{app} (m/s)	Max. shear stress, Γ_{max} (Pa)	Initial shear stress, Γ_o (Pa)
1a	3	0.2	1	1.8231	1.259
1b	3	0.5	1	1.6718	1.259
1c	3.5	0.2	1	1.8805	1.259
1d	3.5	0.5	1	1.78135	1.259
1e	4	0.2	1	2.0346	1.259
1f	4	0.5	1	1.8912	1.259
2a	3	0.2	1.5	3.9299	2.702
2b	3	0.5	1.5	3.595	2.702
2c	3.5	0.2	1.5	4.067	2.702
2d	3.5	0.5	1.5	3.858	2.702
2e	4	0.2	1.5	4.3486	2.702
2f	4	0.5	1.5	3.980	2.702
3a	3	0.2	2	6.7209	4.6429
3b	3	0.5	2	6.037	4.6429
3c	3.5	0.2	2	6.9739	4.6429
3d	3.5	0.5	2	6.374	4.6429
3e	4	0.2	2	7.3845	4.6429
3f	4	0.5	2	6.829	4.6429

By examining the output data, conclusions made are that on increasing the groyne size and approach velocity, maximum shear stress and initial shear stress increases.

Table 12-For position A (UPSTREAM ARC)

GROYNE	Length of groyne, L (m)	Width of groyne (m)	Approach velocity V_{app} (m/s)	Protected length, D (m)	D/L	L/B
1a	3	0.2	1	65.63	21.876	0.15
1b	3	0.5	1	75.323	25.107	0.15
1c	3.5	0.2	1	70.514	20.1468	0.175
1d	3.5	0.5	1	73.748	21.0708	0.175
1e	4	0.2	1	73.964	18.491	0.2
1f	4	0.5	1	75.939	18.9847	0.2
2a	3	0.2	1.5	87.46	29.1533	0.15
2b	3	0.5	1.5	74.313	24.771	0.15
2c	3.5	0.2	1.5	72.468	20.7051	0.175
2d	3.5	0.5	1.5	78.12	22.32	0.175
2e	4	0.2	1.5	86.42	21.605	0.2
2f	4	0.5	1.5	76.179	19.0447	0.2
3a	3	0.2	2	78.92	26.3066	0.15
3b	3	0.5	2	76.93	25.6433	0.15
3c	3.5	0.2	2	75.75	21.6428	0.175
3d	3.5	0.5	2	79.58	22.7371	0.175
3e	4	0.2	2	78.42	19.605	0.2
3f	4	0.5	2	69.38	17.345	0.2

Table 13-For position B (1/4th UPSTREAM ARC)

GROYNE	Length of groyne, L (m)	Width of groyne (m)	Approach velocity V_{app} (m/s)	Protected length, D (m)	D/L	L/B
1a	3	0.2	1	68.467	22.8223	0.15
1b	3	0.5	1	68.83	22.943	0.15
1c	3.5	0.2	1	68.786	19.6531	0.175
1d	3.5	0.5	1	68.68	19.6228	0.175
1e	4	0.2	1	68.72	17.18	0.2
1f	4	0.5	1	68.88	17.22	0.2
2a	3	0.2	1.5	68.637	22.879	0.15
2b	3	0.5	1.5	68.703	22.901	0.15
2c	3.5	0.2	1.5	68.775	19.65	0.175
2d	3.5	0.5	1.5	68.8610	19.6745	0.175
2e	4	0.2	1.5	68.744	17.186	0.2
2f	4	0.5	1.5	68.7209	17.1802	0.2
3a	3	0.2	2	68.644	22.8813	0.15
3b	3	0.5	2	68.885	22.9616	0.15
3c	3.5	0.2	2	68.644	19.6125	0.175
3d	3.5	0.5	2	68.72	19.6342	0.175
3e	4	0.2	2	68.814	17.2035	0.2
3f	4	0.5	2	68.850	17.2125	0.2

Table 14-For position C (1/2 UPSTREAM ARC)

GROYNE	Length of groyne, L (m)	Width of groyne (m)	Approach velocity V_{app} (m/s)	Protected length, D (m)	D/L	L/B
1a	3	0.2	1	49.804	16.601	0.15
1b	3	0.5	1	49.895	16.631	0.15
1c	3.5	0.2	1	49.725	14.207	0.175
1d	3.5	0.5	1	49.829	14.236	0.175
1e	4	0.2	1	49.7711	12.4427	0.2
1f	4	0.5	1	49.91	12.4775	0.2
2a	3	0.2	1.5	49.68	16.56	0.15
2b	3	0.5	1.5	49.853	16.617	0.15
2c	3.5	0.2	1.5	49.61	14.1742	0.175
2d	3.5	0.5	1.5	49.589	14.1682	0.175
2e	4	0.2	1.5	49.844	12.461	0.2
2f	4	0.5	1.5	49.938	12.4845	0.2
3a	3	0.2	2	49.598	16.5326	0.15
3b	3	0.5	2	49.898	16.632	0.15
3c	3.5	0.2	2	49.58	14.1657	0.175
3d	3.5	0.5	2	49.78	14.2228	0.175
3e	4	0.2	2	49.843	12.4607	0.2
3f	4	0.5	2	49.619	12.4047	0.2

As the size of groyne increases, the protected length on the concave face of the river bend also increases. But as the position of groyne changes protected length also changes i.e. as the position

of groyne changes from upstream arc to the middle portion of the arc, protected length of the concave face reduces.

Now having the most efficient size of groyne on the basis of tip velocity and shear stress, the groyne is then installed at different angles w.r.t. the horizontal. The following table gives the values of tip velocity, maximum velocity and protected length at different positions with different velocities.

**Table 15-For position A (upstream arc)
GROYNE L=3, B=0.5, approach velocity=1m/s.**

	Position (in degrees)	V_{max} (m/s)	T_{max} (Pa)	V_{tip} (m/s) (Coordinates)	Protected length(m)
A	$\Theta=15$	1.7738	14.86	0.942 (57.717,52,7.80)	76.980
B	$\Theta=30$	1.7169	14.87	1.402 (56.78,51.45,6.365)	76.854
C	$\Theta=45$	1.5462	16.23	1.234 (56.8,53.93,7.45)	76.5
D	$\Theta=60$	1.4021	16.3	0.957 (58.97,52.98,7.72)	69.632

**Table 16-For position A (upstream arc)
GROYNE L=4, B=0.2, approach velocity=1.5m/s.**

	Position (in degrees)	V_{max} (m/s)	T_{max} (Pa)	V_{tip} (m/s) (Coordinates)	Protected length(m)
A	$\Theta=15$	3.1815	14.87	1.172 (55.86,53.12,6.27)	84.246
B	$\Theta=30$	3.0218	16.428	2.21 (56.1,51.44,6.56)	82.126
C	$\Theta=45$	2.9438	21.33	1.87 (56.82,53.81,6.47)	85.829
D	$\Theta=60$	2.55	19.355	1.788 (54.78,54.68,3.21)	73.8405

Table 17-For position A (upstream arc)
GROYNE L=3, B=0.5, approach velocity=2m/s.

	Position (in degrees)	V _{max} (m/s)	T _{max} (Pa)	V _{tip} (m/s) (Coordinates)	Protected length(m)
A	Θ=15	3.5822	14.8753	0.766 (57.20,51.308,7.715)	77.1916
B	Θ=30	3.5062	16.0305	2.81 (57.30,51.96,6.50)	68.3
C	Θ=45	3.1637	20.56	2.11 (56.82,53.81,6.47)	73.7263
D	Θ=60	2.8209	16.23	2.11 (56.92,53.79,6.46)	69.7803

Table 18-For position B (1/4th upstream arc)
GROYNE L=3, B=0.5, approach velocity=1m/s.

	Position (in degrees)	V _{max} (m/s)	T _{max} (Pa)	V _{tip} (m/s) (Coordinates)	Protected length(m)
a	Θ=15	1.5667	2.80	0.0044 (53.337,31.742,7.67)	78.411
b	Θ=30	1.5871	3.5857	1.086 (53.506,32.6,7.20)	72.248
c	Θ=45	1.5548	3.7987	0.0123 (54.114,33.08,7.628)	73.1683
d	Θ=60	1.4732	3.9990	0.9814 (54.7121,33.7022,7.197)	72.5419

Table 19-For position B (1/4th upstream arc)
GROYNE L=3.5, B=0.5, approach velocity=1.5m/s.

	Position (in degrees)	V _{max} (m/s)	T _{max} (Pa)	V _{tip} (m/s) (Coordinates)	Protected length(m)
a	Θ=15	2.532	7.2202	1.6091 (52.288,32.588,4.525)	75.864
b	Θ=30	2.5805	9.0326	1.657 (52.971,33.046,5.191)	74
c	Θ=45	2.5049	9.5156	1.730 (53.123,33.582,4.527)	75.2085
d	Θ=60	2.368	9.1283	1.5077 (54.495,34.170,7.136)	73.988

**Table 20-For position B (1/4th upstream arc)
GROYNE L=3, B=0.5, approach velocity=2m/s.**

	Position (in degrees)	V _{max} (m/s)	T _{max} (Pa)	V _{tip} (m/s) (Coordinates)	Protected length(m)
a	Θ=15	3.204	10.999	0.9563 (53.77,32.475,7.649)	73.9806
b	Θ=30	3.2413	13.359	1.0885 (53.282,31.848,6.965)	73.954
c	Θ=45	3.1675	14.215	1.656 (53.96,33.14,7.101)	73.69
d	Θ=60	3.015	14.9604	1.496 (54.739,33.64,7.764)	72.039

**Table 21-For position C (1/2 upstream arc)
GROYNE L=3, B=0.5, approach velocity=1m/s.**

	Position (in degrees)	V _{max} (m/s)	T _{max} (Pa)	V _{tip} (m/s) (Coordinates)	Protected length(m)
a	Θ=15	1.3463	2.84	1.0303 (42.88,16.248,5.985)	49.812
b	Θ=30	1.4707	2.8781	1.097 (42.978,17.136,6.652)	49.677
c	Θ=45	1.5185	3.523	1.0754 (43.595,17.64,6.902)	48.0121
d	Θ=60	1.5218	3.6271	0.9645 (44.207,18.607,6.372)	48.223

**Table 22-For position C (1/2 upstream arc)
GROYNE L=3, B=0.5, approach velocity=1.5m/s.**

	Position (in degrees)	V _{max} (m/s)	T _{max} (Pa)	V _{tip} (m/s) (Coordinates)	Protected length(m)
a	Θ=15	2.0217	5.675	1.4502 (42.91,15.996,7.647)	49.998
b	Θ=30	2.2187	6.1803	1.6007 (43.184,16.8704,7.259)	49.779
c	Θ=45	2.299	7.592	1.5504 (43.375,18.1304,6.108)	49.9075
d	Θ=60	2.2988	7.844	1.5450 (44.325,18.026,7.400)	49.9429

**Table 23-For position C (1/2 upstream arc)
GROYNE L=3, B=0.5, approach velocity=2m/s.**

	Position (in degrees)	V _{max} (m/s)	T _{max} (Pa)	V _{tip} (m/s) (Coordinates)	Protected length(m)
a	Θ=15	2.7006	9.73697	2.063 (42.932,16.069,7.539)	49.8095
b	Θ=30	2.9750	10.6299	2.1417 (43.039,17.129,7.298)	49.952
c	Θ=45	3.0829	13.093	2.313 (43.657,17.770,5.715)	49.6549
d	Θ=60	3.0785	13.573	1.880 (44.384,18.26,6.641)	49.7848

For position ‘A’, as the angle of installation increases from 15° to 60° for a fixed groyne size at different velocities, maximum velocity decreases and maximum shear stress increases.

For position ‘B’, as the angle of installation increases from 15° to 60° for a fixed groyne size at different velocities, maximum velocity has a sudden rise for angle 30° and then decreasing values are obtained. Maximum shear stress increases with the increase in installation angle.

For position ‘C’, as the angle of installation increases from 15° to 60° for a fixed groyne size at different velocities, maximum velocity increases and maximum shear stress increases following the above trend.

4.3. PLOTS OBTAINED FROM ANSYS FLUENT (CFD –POST)

The results below are for position A of groyne in the channel. All the plots are for the most efficient groyne size for different velocities. The flow is taking place from right to left.

The groyne size for each case shown here is different and plots obtained are for velocity 1 m/s.

4.3.1. STREAMLINES

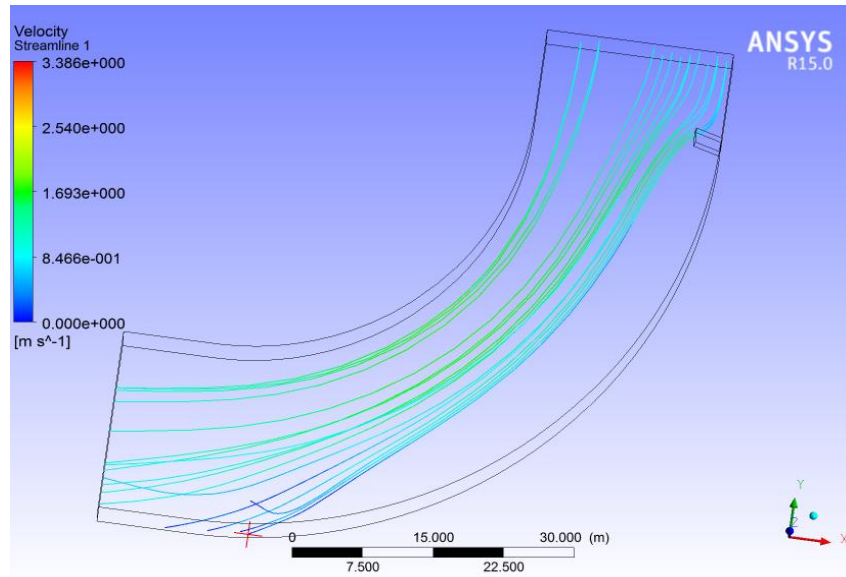


Fig. No. 10 Streamlines for groyne position “A” having groyne at 15° , with respect to decided meridian “OA”.

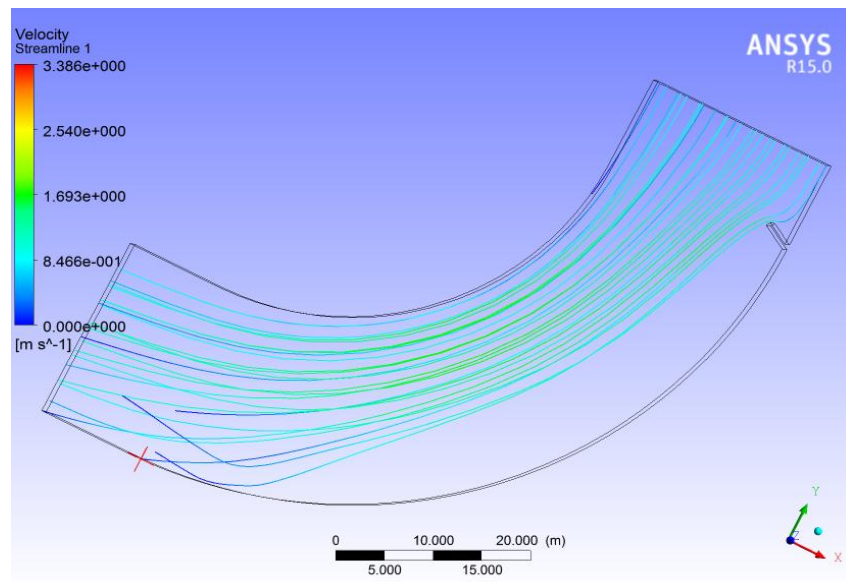


Fig. No. 11 Streamlines for groyne position “A” having groyne at 30° , with respect to decided meridian “OA”.

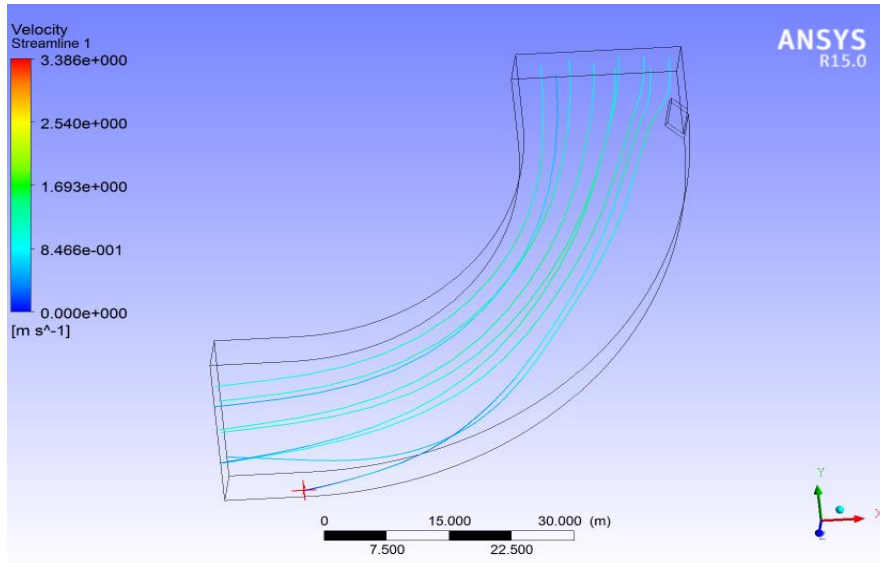


Fig. No. 12 Streamlines for groyne position “A” having groyne at 45°, with respect to decided meridian “OA”.

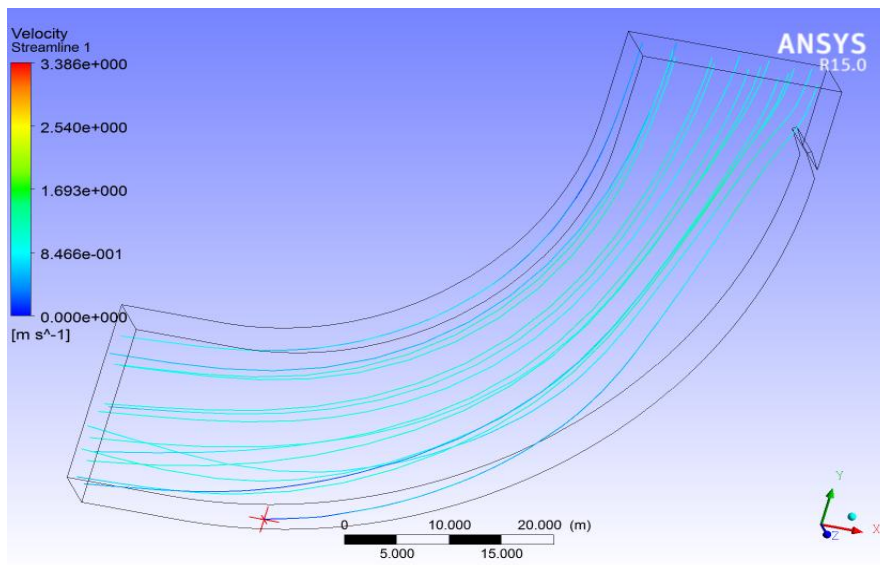


Fig. No. 13 Streamlines for groyne position “A” having groyne at 60°, with respect to decided meridian “OA”.

4.3.2. VELOCITY VECTORS

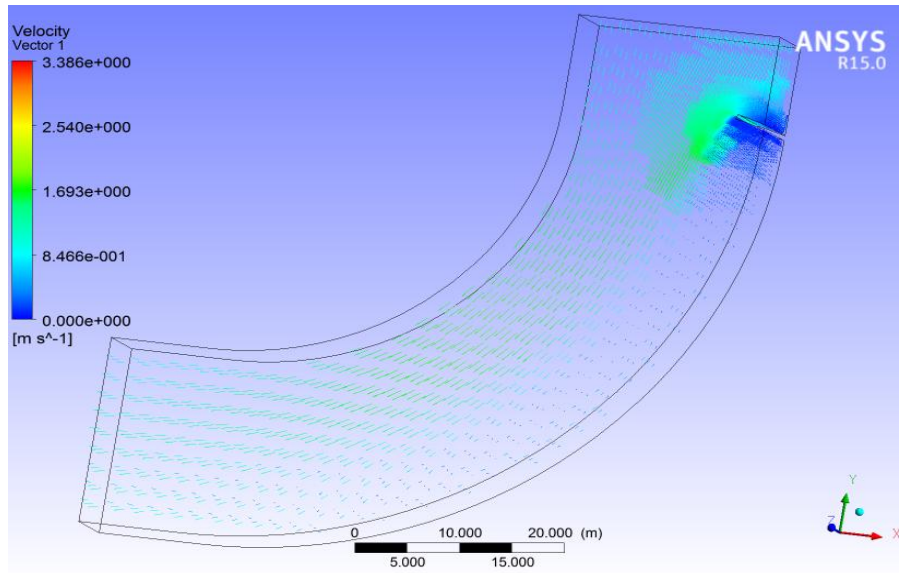


Fig. No. 14 Velocity Vectors for groyne position “A” having groyne at 15° , with respect to decided meridian “OA”.

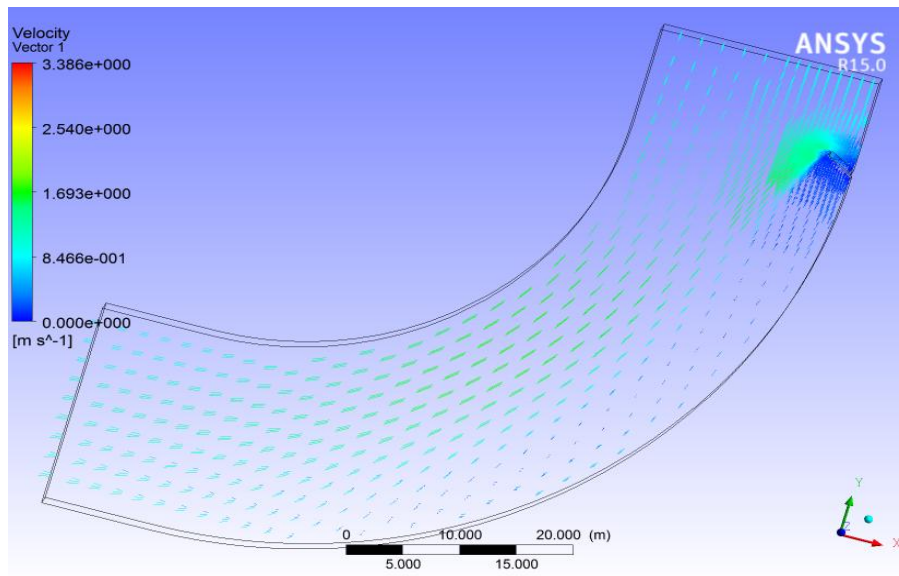


Fig. No. 15 Velocity Vectors for groyne position “A” having groyne at 30° , with respect to decided meridian “OA”.

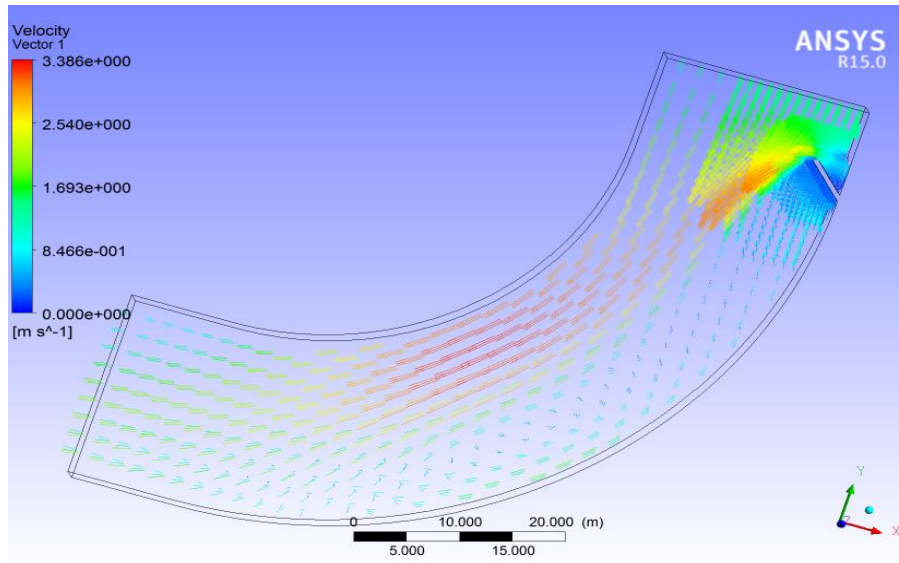


Fig. No. 16 Velocity Vectors for groyne position “A” having groyne at 45°, with respect to decided meridian “OA”.

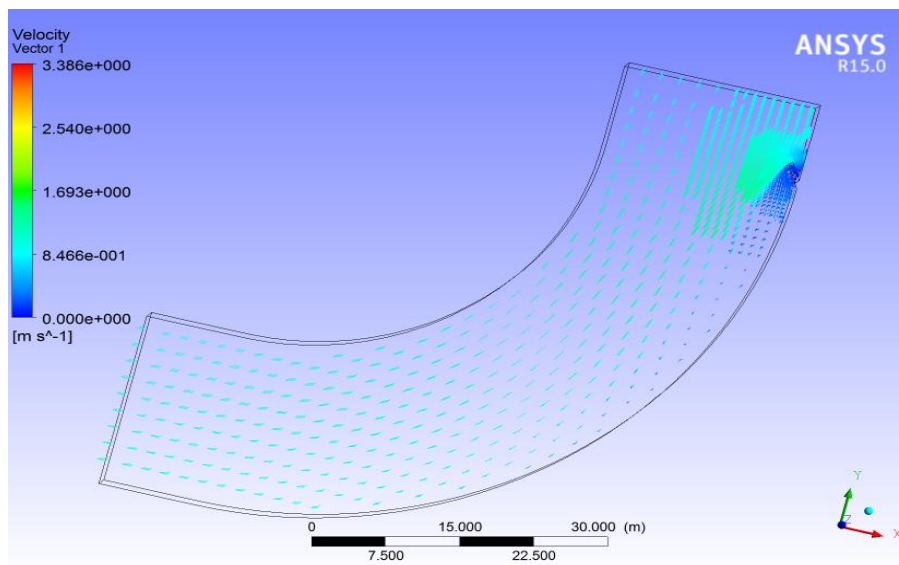


Fig. No. 17 Velocity Vectors for groyne position “A” having groyne at 60°, with respect to decided meridian “OA”.

4.3.3. CONTOURS OF VELOCITY

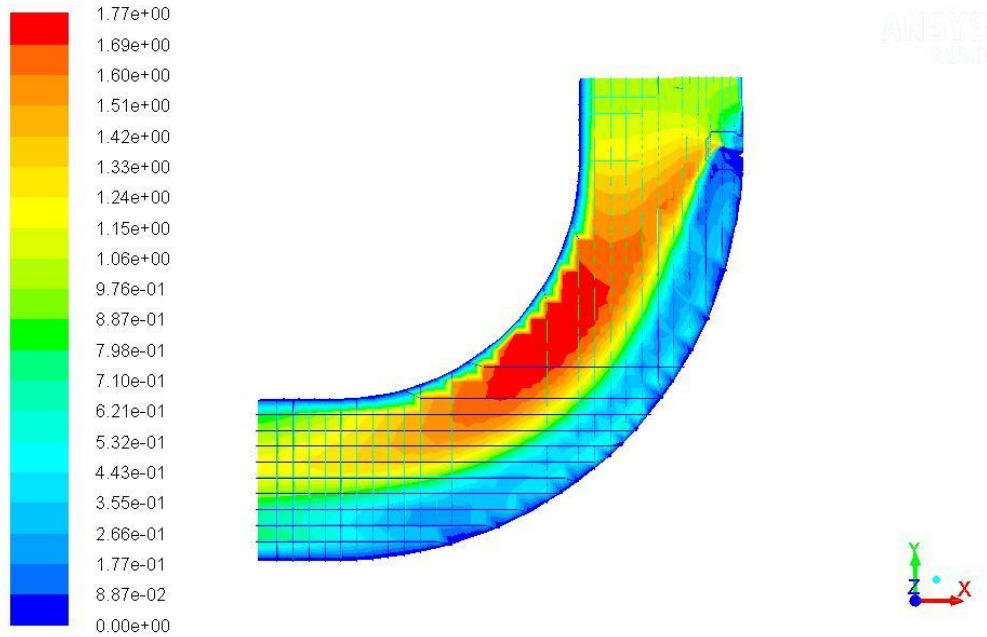


Fig. No. 18 Velocity Contours for groyne position “A” having groyne at 15°, with respect to decided meridian “OA”.

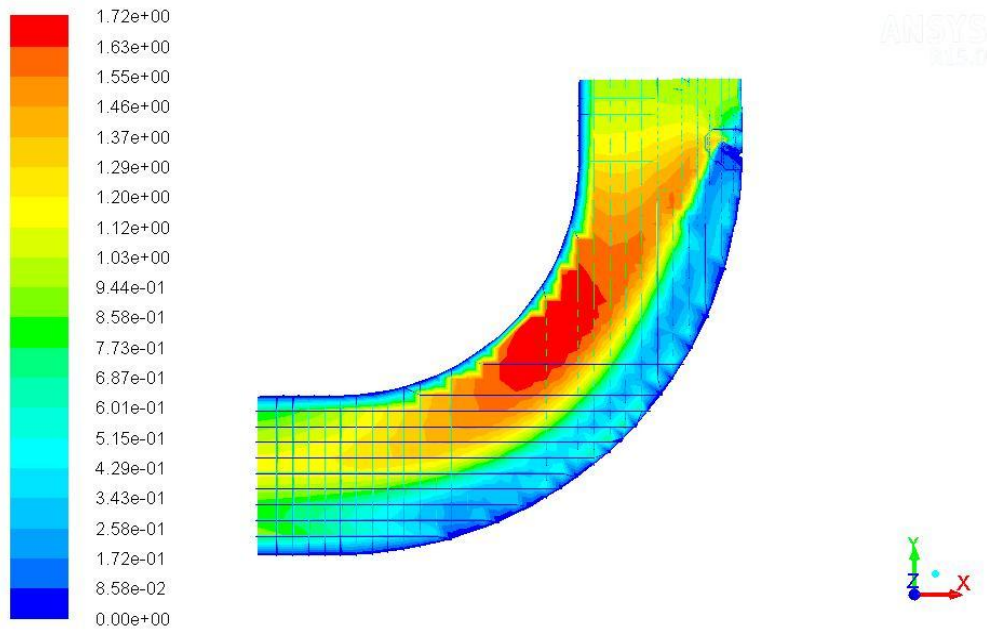


Fig. No. 19 Velocity Contours for groyne position “A” having groyne at 30°, with respect to decided meridian “OA”.

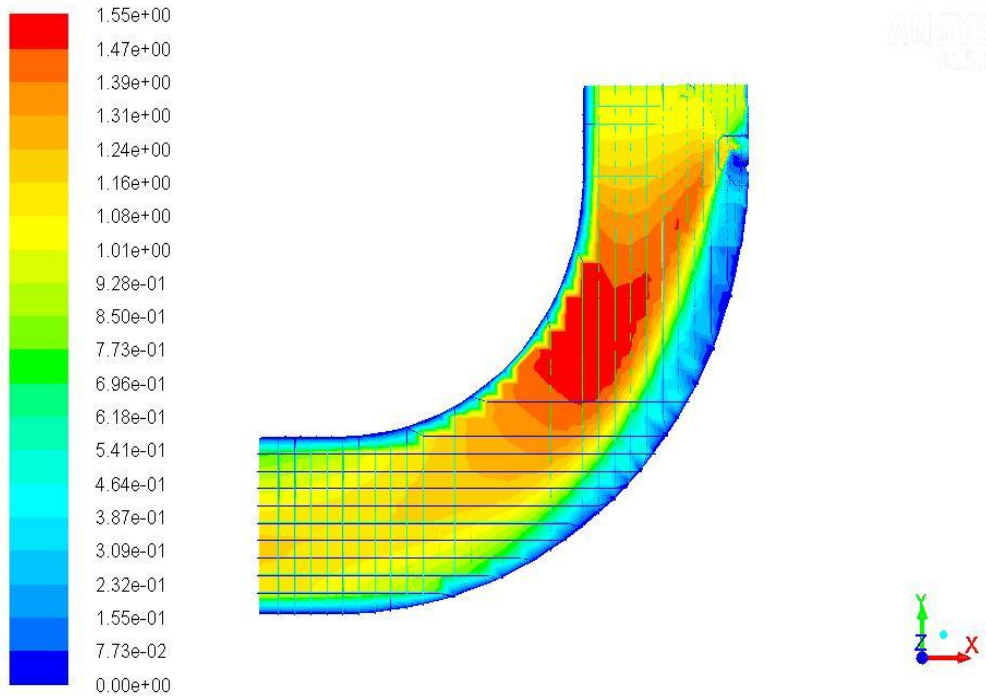


Fig. No. 20 Velocity Contours for groyne position “A” having groyne at 45°, with respect to decided meridian “OA”.

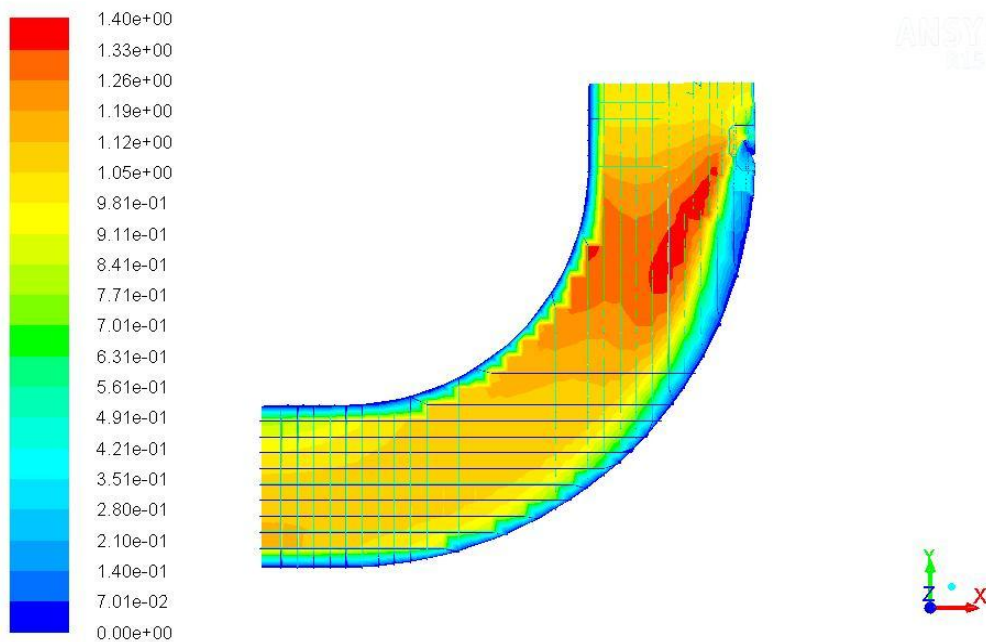


Fig. No. 21 Velocity Contours for groyne position “A” having groyne at 60°, with respect to decided meridian “OA”.

4.3.4. CONTOURS OF BED SHEAR STRESS

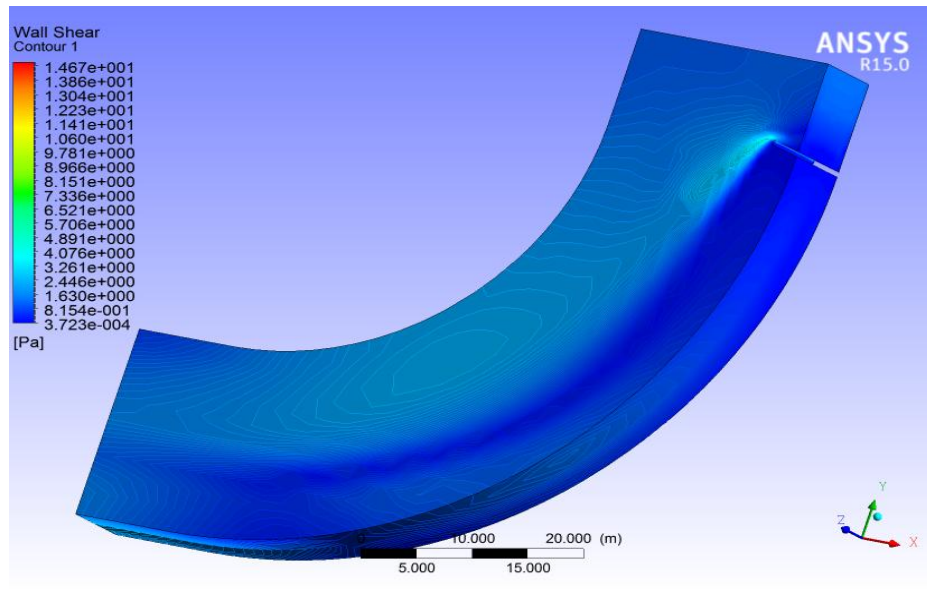


Fig. No. 22 Bed Shear Stress Contours for groyne position “A” having groyne at 15° , with respect to decided meridian “OA”.

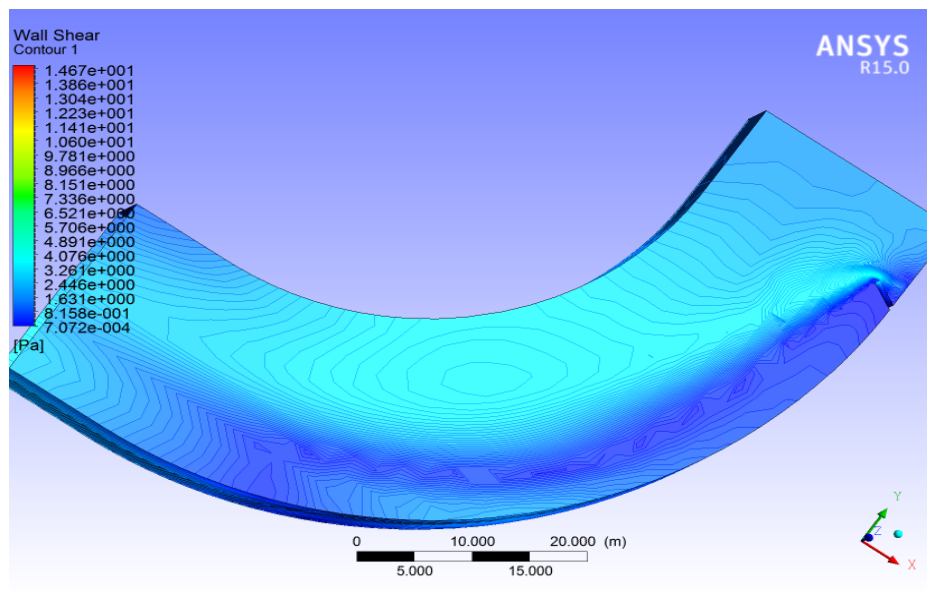


Fig. No. 23 Bed Shear Stress Contours for groyne position “A” having groyne at 30° , with respect to decided meridian “OA”.

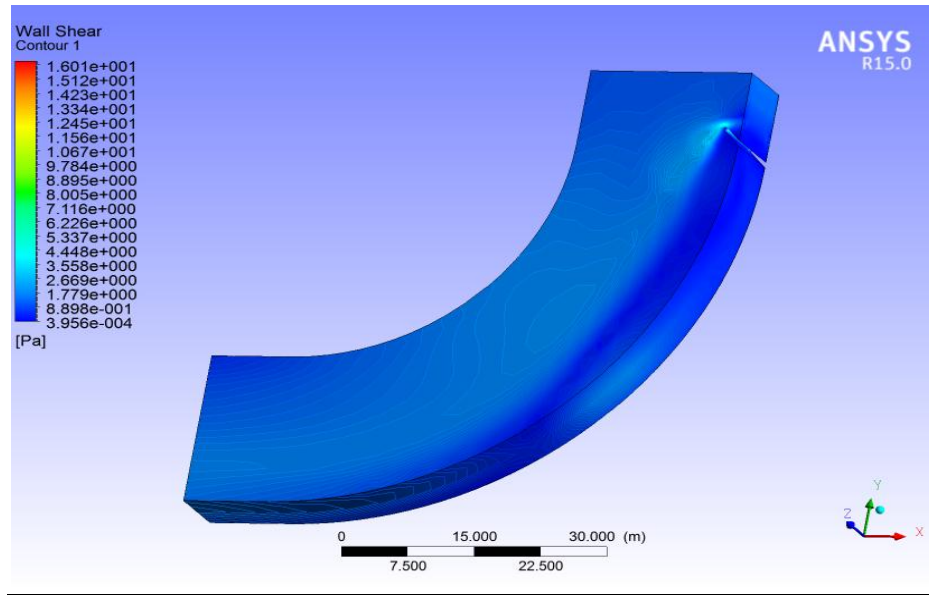


Fig. No. 24 Bed Shear Stress Contours for groyne position “A” having groyne at 45°, with respect to decided meridian “OA”.

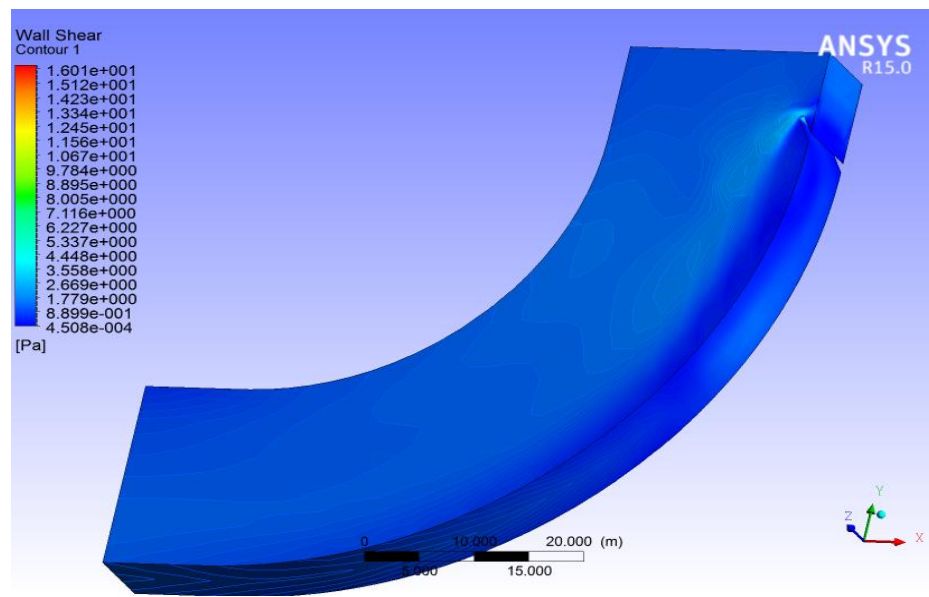


Fig. No. 25 Bed Shear Stress Contours for groyne position “A” having groyne at 60°, with respect to decided meridian “OA”.

The aim of this study was to find the best placement and size of groyne in a channel bend. There are a number of factors that influence the complex flow which takes place in a channel bend. Though introduction structures like groyne, spurs or guide banks helps in training the river, they simultaneously make the analysis of the river regime more difficult. It is not possible to predict all the factors that are affecting the flow and how much is their contribution, so an attempt is made to analyze the factors.

The major factors that can be thought to predict the flow around groyne in a bend are namely-

- a) Maximum Shear Stress
- b) Velocity near the tip of the groyne or Tip velocity
- c) Groyne Size
- d) Protection length, that is the length of bank protected due to the introduction of groyne on the concave face
- e) Froude Number
- f) Radius of Bend
- g) Absolute maximum velocity

Thus, from the various observation on different groyne size and their position, an appreciable relation between different factors was found.

4.4. VARIATION OF FACTOR D/L WITH FACTOR L/B FOR DIFFERENT POSITION OF THE GROYNES.

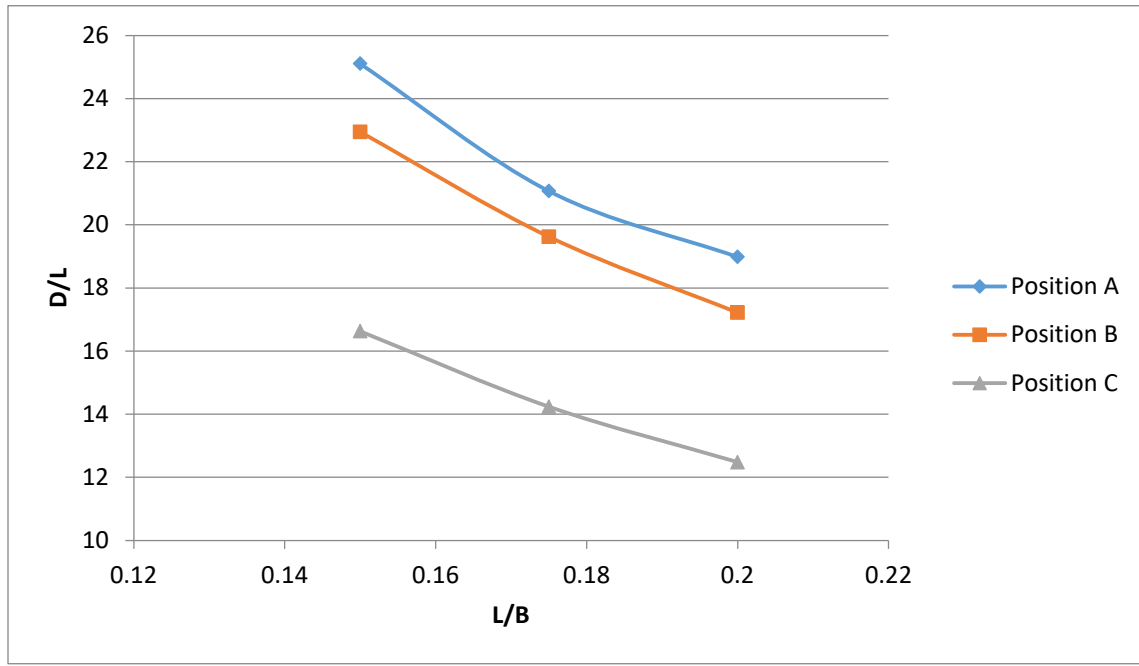


Fig. No. 26 Variation of D/L with L/B for Velocity 1m/s

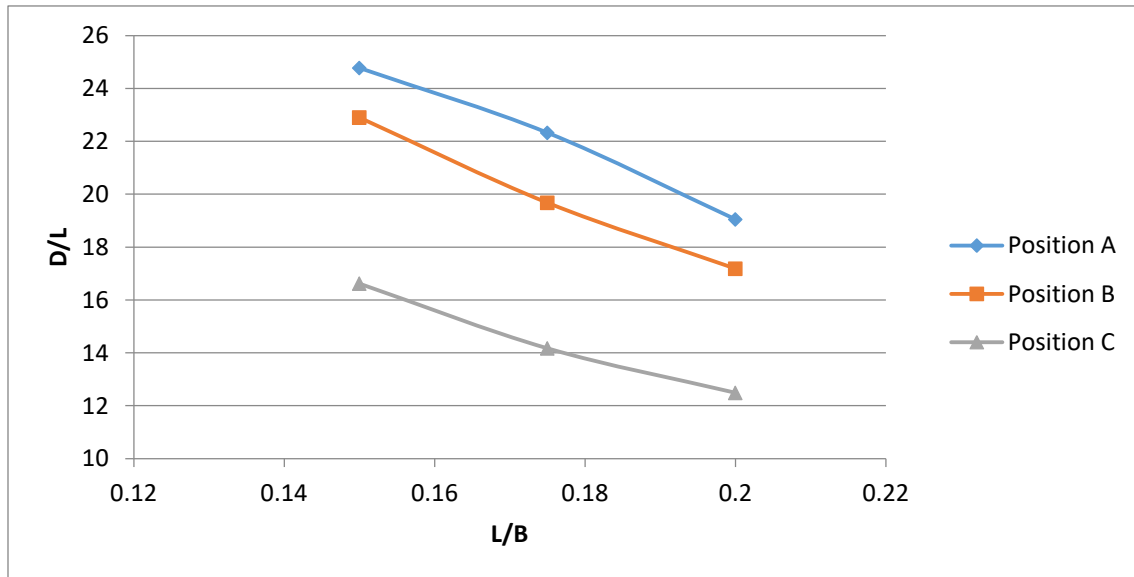


Fig. No. 27 Variation of D/L with L/B for Velocity 1.5m/s

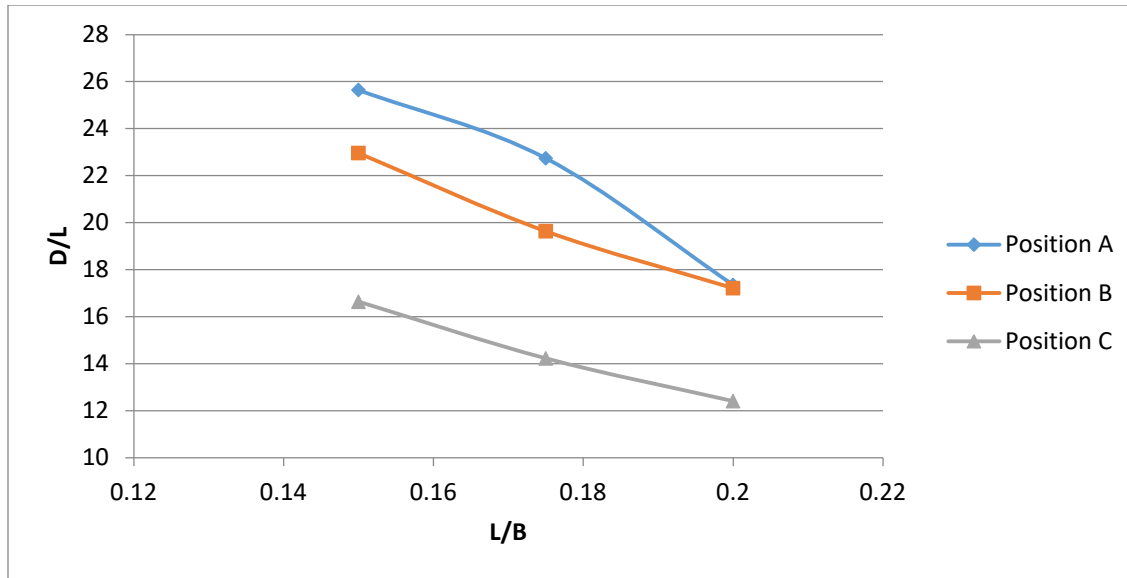


Fig. No. 28 Variation of D/L with L/B for Velocity 2m/s

It can be observed that the variation is not linear, as expected there are other factors that influence the Protection Length. It can be inferred from the variation that with increase in L/B ratio the value of D/L decreases for almost all the cases of placement of groyne. Protection length is maximum for position A for all the groyne sizes at all velocities and a good protection length is obtained for position B.

4.5. VARIATION OF FACTOR L/B WITH FACTOR V_{tip}/V_{app} FOR DIFFERENT POSITION OF THE GROYNES.

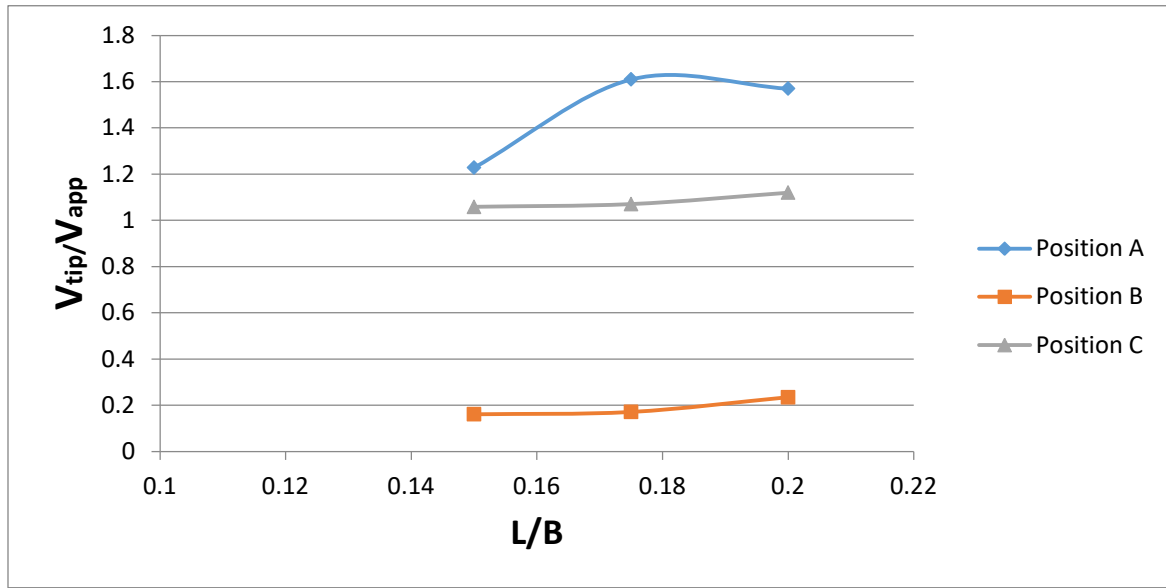


Fig. No. 29 Variation of V_{tip}/V_{app} with L/B for Velocity 1 m/s.

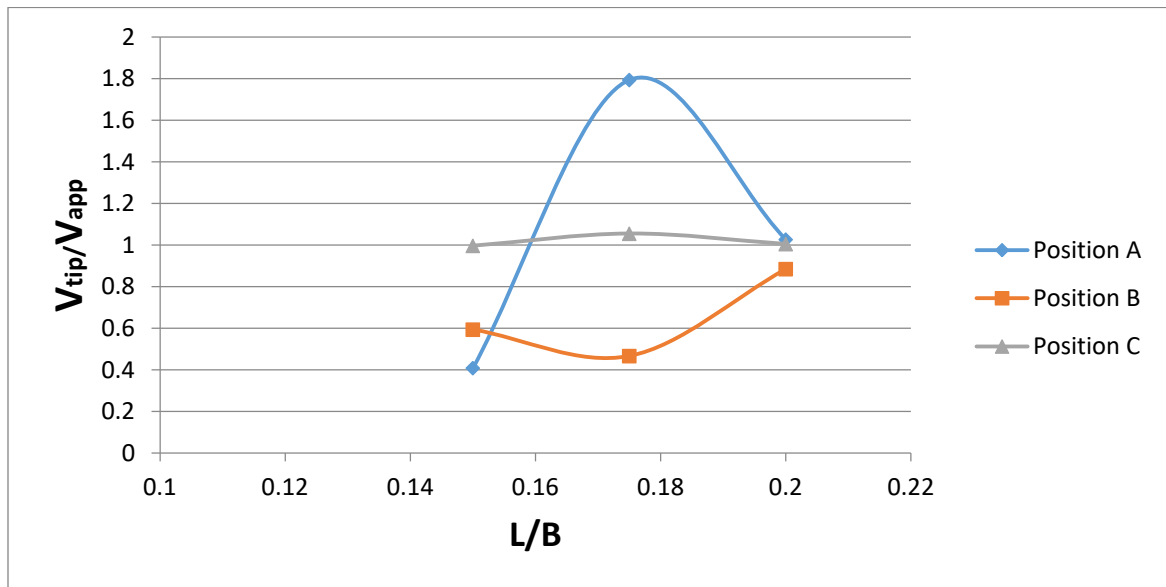


Fig. No. 30 Variation of V_{tip}/V_{app} with L/B for Velocity 1.5 m/s.

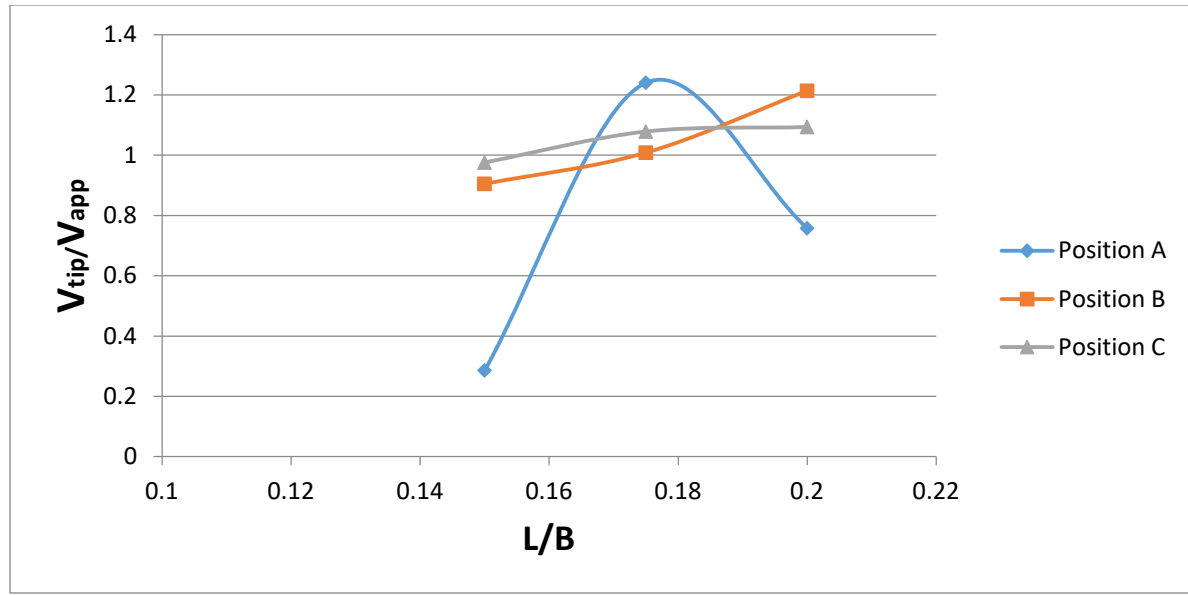


Fig. No. 31 Variation of V_{tip}/V_{app} with L/B for Velocity 2 m/s.

It can be observed that the variation is not linear, as expected there are other factors that influence the Tip Velocity. It can be concluded from the variation that with increase in L/B ratio the value of V_{tip}/V_{app} increases for more of the cases of placement of groyne at different positions.

The position that should be noted is position A, for an L/B ratio of 0.175, that is Length of groyne=3.5m. At this position for all the velocities of flow it can be seen that there is sudden drop in the V_{tip}/V_{app} factor or the tip velocity. The tip velocity and the maximum velocity are found near the groyne and thus it contributes to the formation of vortices that lead to scouring.

Owing to the curvature of the section it can be seen that the velocities here also contribute to the production of centrifugal forces on the bend which in turn will cause more scouring. Free vortex is formed where the curvature is more and where the tip velocity is maximum thus creating more disturbances as that might be observed in a straight channel.

It should also be noted that the position of this tip velocity is very near to the position of maximum bed shear stress. Thus variation of shear stress was also needed to be studied, as the above analysis cannot on its own determine a good placement.

4.6. VARIATION OF FACTOR τ_{\max} FOR DIFFERENT GROUYNE POSITION.

- For position A i.e. upstream arc

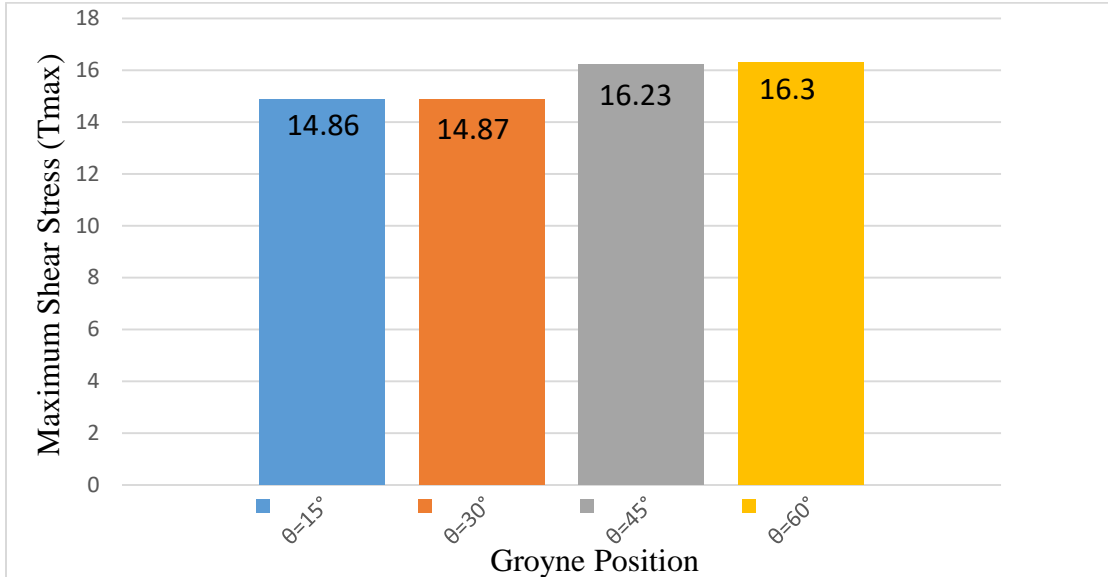


Fig. No. 32 τ_{\max} for groyne size L=3m, B=0.5 for velocity 1m/s

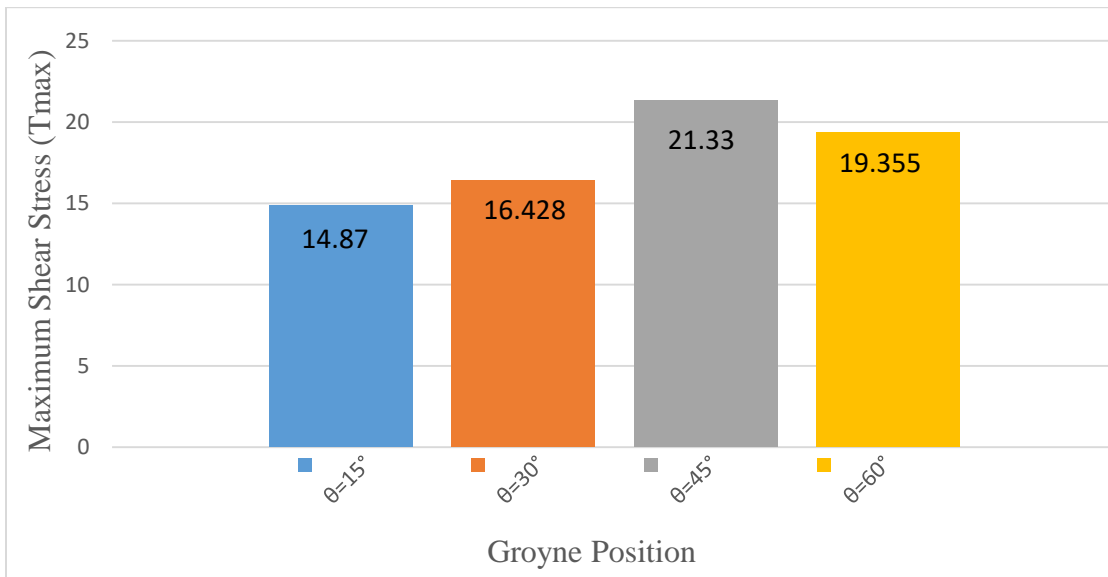


Fig. No. 33 τ_{\max} for groyne size L=3m, B=0.5 for velocity 1.5m/s

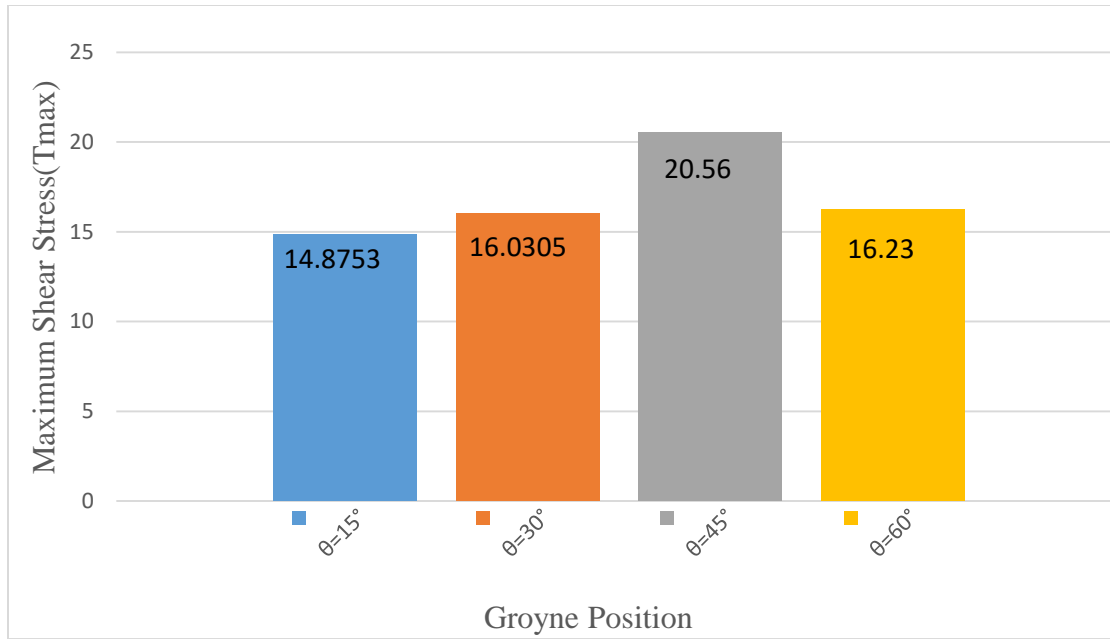


Fig. No. 34 τ_{\max} for groyne size L=3m, B=0.5 for velocity 2m/s

- **For position B i.e. 1/4th upstream arc**

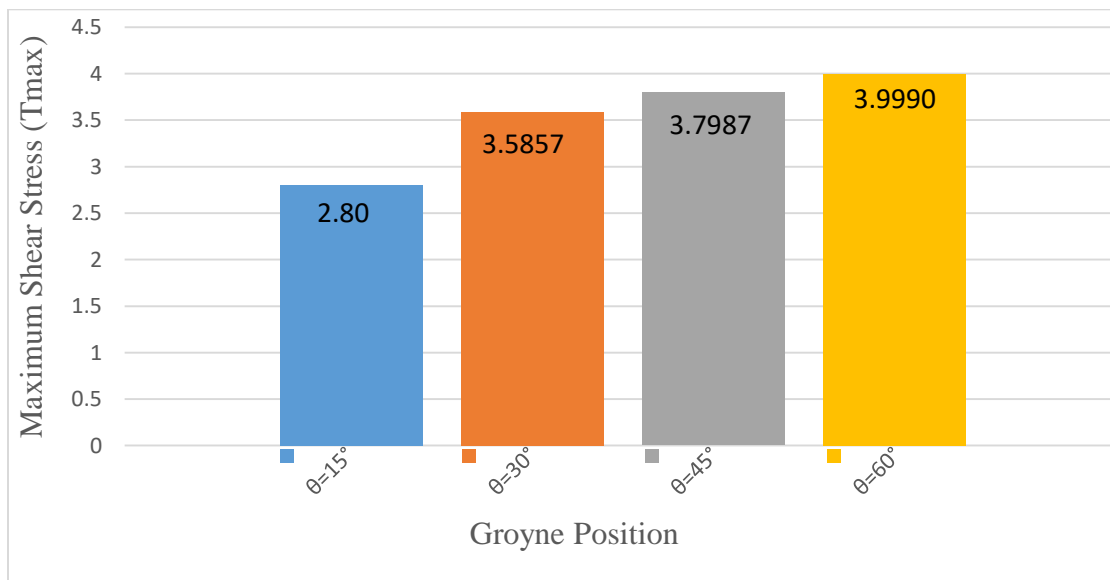


Fig. No. 35 τ_{\max} for groyne size L=3m, B=0.5 for velocity 1m/s

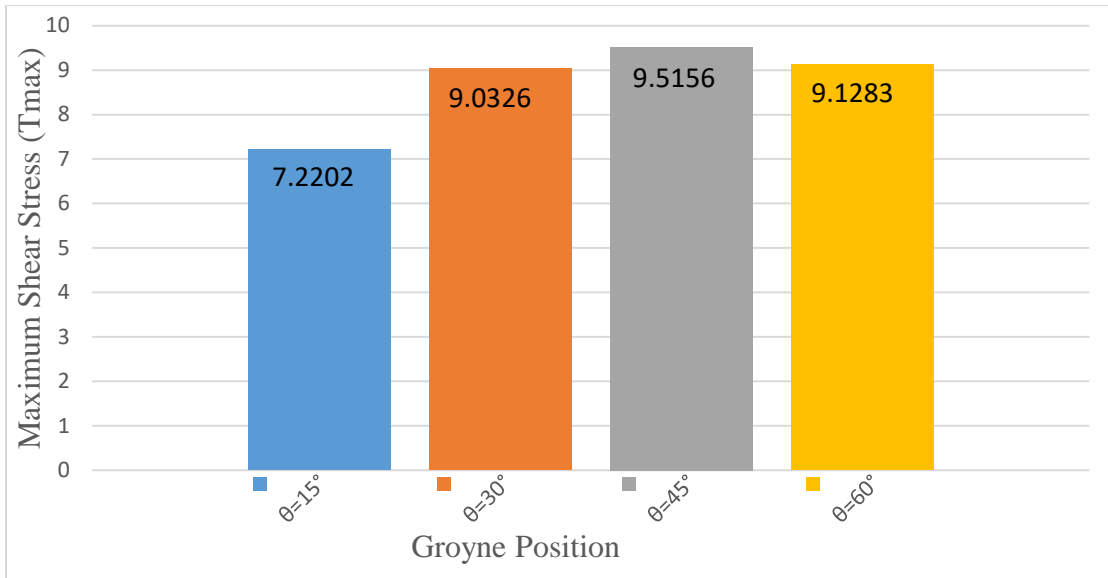


Fig. No. 36 τ_{max} for groyne size $L=3m$, $B=0.5$ for velocity $1.5m/s$

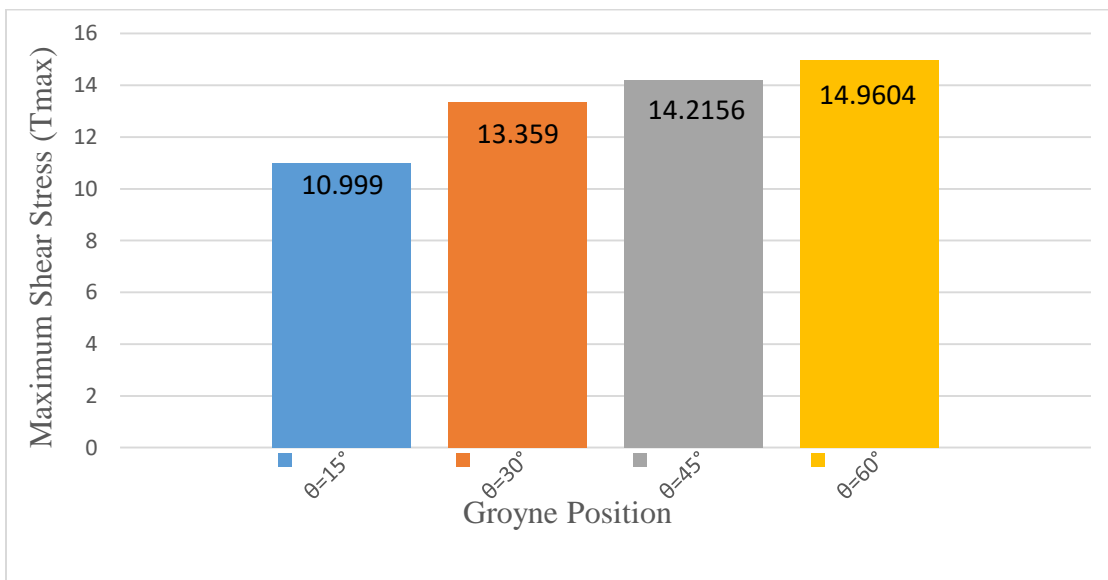


Fig. No. 37 τ_{max} for groyne size $L=3m$, $B=0.5$ for velocity $2m/s$

- **For position C i.e. ½ upstream arc**

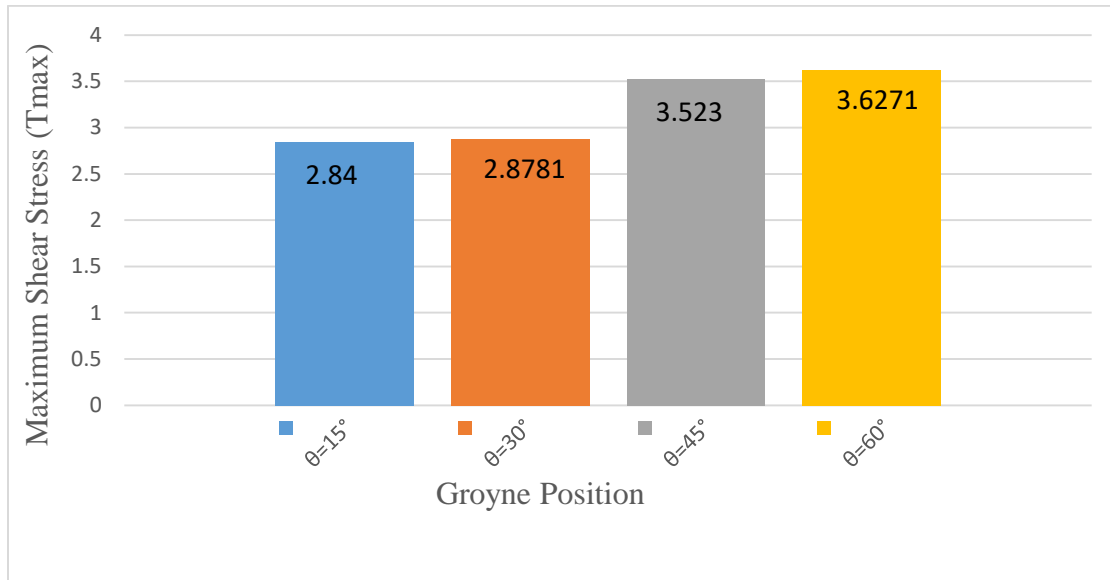


Fig. No. 38 τ_{max} for groyne size $L=3m$, $B=0.5$ for velocity $1m/s$

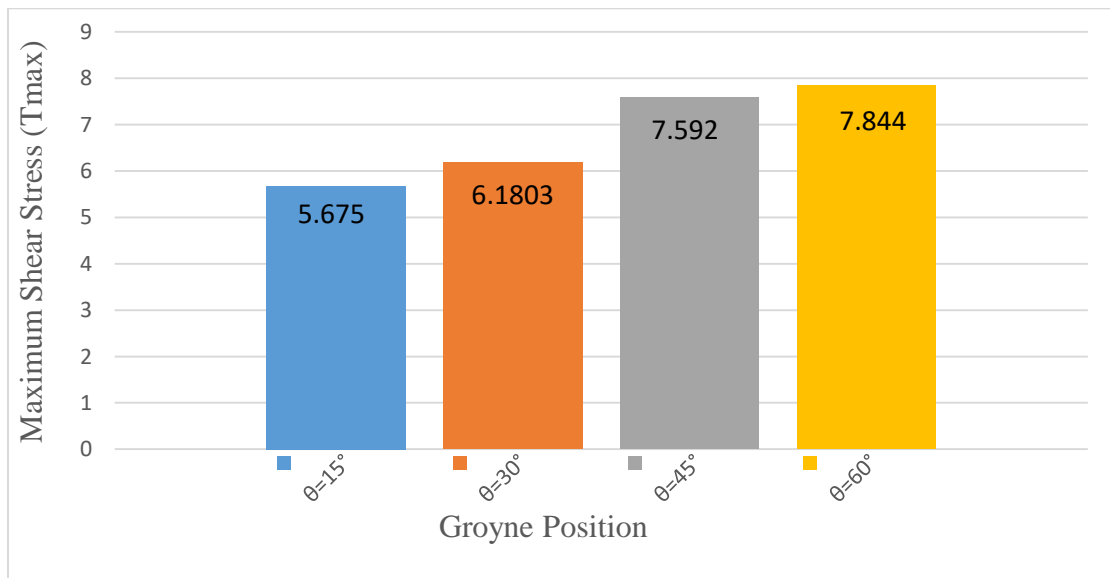


Fig. No. 39 τ_{max} for groyne size $L=3m$, $B=0.5$ for velocity $1.5m/s$

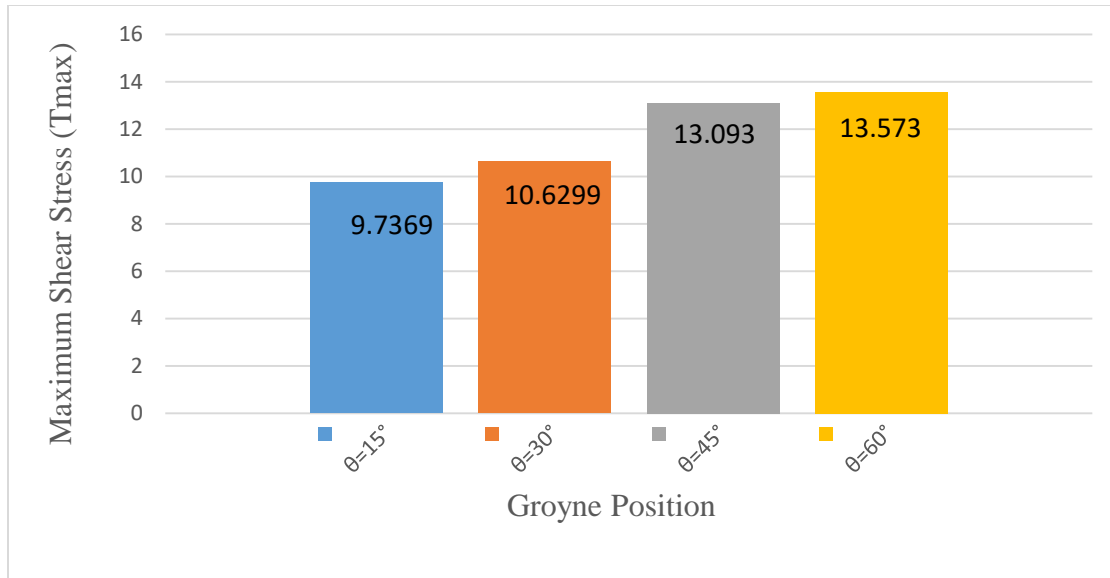


Fig. No. 40 τ_{\max} for groyne size $L=3\text{m}$, $B=0.5$ for velocity 2m/s

Analysis of the above variation shows that the maximum shear stress increases with increase in installation angle of groyne for almost all the velocities. Thus a maximum value of 21.33 Pa for velocity 1.5m/s was observed for groyne size of 3m at position A and minimum shear stress of 2.80 Pa for velocity of 1m/s at position B. It can also be seen that in each case for various velocities the minimum value occurs at position 'a'. This shows that this position is the most efficient i.e. at angle $\theta=15^\circ$ among all the position for all velocities.

4.7. SUMMARY

The above analysis of factors that affect the flow in a channel bend gives an idea of which position or placement of groyne is the most efficient. The position 'a' of groyne that is placed at an angle of 15° with respect to decided meridian "OA" on $1/4^{\text{th}}$ upstream arc is the most efficient position as the maximum shear stress is found to be minimum at this position, tip velocity at the groyne is also relatively very low and Protected length is also good at different approach velocities considered. Thus on the basis of the above studies it is the best placement of groyne to pass the flow through the channel bend safely and protect the concave face from erosion.

Suggestion for the groyne size can be also given based on the trend seen in the various factors during the iterations. Groyne size of length 3.5m and width 0.5m gives considerable good results when employed at position "B" i.e. on $1/4^{\text{th}}$ upstream arc in this channel bend.

CHAPTER 5

CONCLUSIONS

5.1. INTRODUCTION

This chapter indexes the conclusions that are made based on analysis of the results obtained and the relationship derived among the various factors involved. The factors that are understood to be most important for the complex flow in a channel bend are mentioned below.

After sincere analysis of the inferences and the data obtained, the best placement of groyne is also predicted, that protects the bend in the most efficient way.

1. The **tip velocity** is the velocity near the tip of the groyne on the concave bank. This velocity has significance to understand local scouring, its extent and location.

It is seen that the variation of factor V_{tip}/V_{app} is increasing with increase in groyne size. It can be inferred from the variation between V_{tip}/V_{app} and L/B that the minimum values of tip velocity ratio is for position 'A' (upstream arc) and position 'B' (1/4th upstream arc). Thus in concurrence with the above inference, position 'A' (upstream arc) and 'B' (1/4th upstream arc) is the more efficient positions among others. It can also be seen from the variation of V_{tip}/V_{app} vs. L/B that there is a drop in the value of tip velocity ratio at position 'B' and this is very close to the absolute minimum value of V_{tip}/V_{app} for any position.

Thus we can say that out of position 'A' (upstream arc) and position 'B' (1/4th upstream arc), the position 'B' is more efficient.

Also, it can be noted that this minimum value occurs at L/B ratio of 0.175 that is for groyne size of 3.5m.

2. **Maximum bed shear stress** is a critical factor for the flow in a channel bend. This helps in scouring and its extent that will take place. The bed shear stress in this study was found to be maximum always near the groyne, thus suggesting the location of local scour.

As expected the value of maximum shear stress reduces as the approach velocity varied from 2m/s;1.5m/s to 1m/s. Though the relation with the different positions of the groyne was not linear and local minimum, local maximum was found in the data. For location 'a' (groyne placed at an angle of 15°) the minimum value of bed shear stress was found among all the position of groyne placement for different velocities. This suggests that the

placement 'a' (groyne placed at an angle of 15°) is the most effective among the other positions.

3. The **protected length (D)**, which is the length of the concave bend of the section that was protected after the introduction of the groyne is an important factor for the flow. The variation of this factor can in itself throw some light on the placement of groyne that is giving the best results.

It is seen that the protected length depends on the position of the groyne. Through the relationship or variation is not linear, the maximum value of 'D' is observed for position 'A' (upstream arc) and position 'B' ($1/4^{\text{th}}$ upstream arc).

Where, $D(\text{position 'A'}) > D(\text{position 'B'})$ for all velocities 1m/s; 1.5m/s; 2m/s.

This analysis helps us narrow down our field of vision to choose the best placement, to position A (upstream arc) or position B ($1/4^{\text{th}}$ upstream arc).

5.2. SUGGESTION FOR THE BEST PLACEMENT OF GROUYNE.

After analysis of the factors involved, an efficient placement of groyne can be established with an appreciable confidence.

The position "a" that is groyne placed at an angle of 15° with respect to decided meridian "OA" at position "B" ($1/4^{\text{th}}$ upstream arc) is the most efficient placement among all the positions. This position gives the minimum value of bed shear stress and tip velocity simultaneously providing a high value of protected length over concave bank.

Also certain suggestion can be given for the appropriate length of the groyne. The factors maximum shear stress, tip velocity and protected length are found to in appreciable range for L/B ratio of 0.175 that is groyne size of 3.5m and width 0.5m.

5.3. FURTHER IMPROVEMENTS

- a) The width of the channel and Radius of curvature of bend can also be varied to get more variations and derive factors to get better results.
- b) Different models for analysis can be applied that are available in Ansys Fluent like Large Eddy Simulation, which may give better results.

REFERENCES

1. Suharjoko, 2001, "Numerical Modeling of Two-Dimensional Horizontal Flow on Groyne Field due to Groyne Placement on the River Straight", Researches Report, Department of Research and Applications, Institute of Technologie Sepuluh Nopember, Surabaya, 2001.
2. Suharjoko, "Study on Numerical Modeling of Two-Dimensional Horizontal Flow special case Groyne on the River Estuary", Thesis for the degree of Master Science in Civil Engineering Program, Department of Engineering Science, Post-graduate Program, University Of Gajah Mada, Yogyakarta, 1999.
3. Kashyap, Shalini. "NUMERICAL MODELING OF FLOW AROUND SUBMERGED GROYNES IN A SHARP BEND USING LARGE EDDY SIMULATION". Diss. University of Ottawa, 2010.
4. Jungseok Ho, Hong Koo Yeo, Julie Coonrod, and Won-Sik Ahn, "NUMERICAL MODELING STUDY FOR FLOW PATTERN CHANGES INDUCED BY SINGLE GROUYNE", Seminario Internacional La Hidroinformática en la Gestión Integrada de los Recursos Hídricos, Universidad del Valle/Instituto Cinara Kutija, V. and Murray, M. G. 162 , 2005.
5. Prohaska Sandra (2007), Thomas Jancke, Bernhard Westrich, "MODEL BASED ESTIMATION OF SEDIMENT EROSION IN GROUYNE FIELDS ALONG THE RIVER ELBE", University of Stuttgart, Institute of Hydraulic Engineering, Stuttgart, Germany, 2006.
6. Zhang Hao, Hajime Nakagawa, Yasunori Muto, Yosio Muramoto, et al, "Morphodynamics of Channel with Groins its Applications in River Restoration", Annual of Disas, Prev. Res. Inst. Kyoto Univ., No. 50 B. 2007.
7. Zhang Hao, Mizutani and Nakagawa, "Impact of Grain Size Distribution on Bed Topography around a Groyne", 34th IAHR worl Congress – Balance and Uncertainty, ISBN 978-0-85825-868-6, Brisbane, Australia, 26 June-1 July 2011.
8. FLUENT user's guide manual-version 6.3.26. Fluent Inco.
9. "Numerical Simulation of the Angle of Groyne Installation on the Separation Zone Length Behind it", by Hamid Shamloo and Bahareh Pirzadeh, Associate Professor at K.N. Toosi University of Technology.

10. Nagata, N., Hosoda, T., Nakato, T. and Muramoto, Y. "Three-dimensional numerical model for flow and bed deformation around river hydraulic structures", *J. Hydraulic. Eng., ASCE*, Vol.131. No.12, 2005, pp.1074-1087.
11. Nur Yuwono, *Hydraulics Modeling*, Central of University Association on Engineering Science, University Of Gajah Mada, Yogyakarta., 1994.
12. Armani A, M. Righety, Sartori F, "Experimental Analysis of Fluvial Groyne", *Proc, of River Flow*, Braunschweig, (2010).
13. Krishna Prasad, S. Indulekha, Balan. K, "Analysis of groyne placement on minimizing river bank protection", *College of Engineering Trivandram* (2015).
14. J. Yajdi, H. Sarkardeh, Aminuddin N. Ghani, "3D Simulation flow around a single spur dike with free-surface flow", *Water Research Institute*, 2010.
15. Suharjoko, Mohammad Bisri, Rispiningtati, Muhammad Ruslin Anwar, "An Analysis Of The Groyne Placement At The River Bend Based On Current Flow Be Occurred", *Brawijaya University*, Malang.
16. Mohammad Vaghefi; Masoud Ghodsian; and Seyed Ali Akbar Salehi Neyshabouri, "Experimental Study on Scour around a T-Shaped Spur Dike in a Channel Bend", *Persian Gulf Univ., Bushehr, Iran*, 2012.
17. Mohammad Vaghefi, Masoud Ghodsian, Maryam Akbari, "Experimental Investigation on 3D Flow around a Single T-Shaped Spur Dike in a Bend", *Persian Gulf University*, 2016.
18. S. A. Salamatian, M. Forghani, and M. Karimae Tabarestani, "Flow Pattern and Stress Distribution around Three Spur Dike in Ninety Degree Bend", *Tarbiat Modares University, Tehran, Iran*, 2015.
19. Majid FAZLI, Masoud GHODSIAN, and Seyed Ali Akbar Salehi NEYSHABOUR, "Scour and flow field around a spur dike in a 90° bend", *Tarbiat Modares University, Tehran, Iran*, 2008.
20. A.R.Masjedi, H.Moradi, "Experimental Research effect of spur dike position on the depth of scouring in the rivers Bend 180 deg", *.Islamic Azad University,Ahwaz,Iran*, 2008.
21. Hassan Safi AHMED, Mohammad Mahdi HASAN, Norio TANAKA, "Analysis of flow around impermeable groynes on one side of symmetrical compound channel: An experimental study", *South Valley University, Qena 83521, Egypt*, 2009.